



---

# European Reviews of Chemical Research

---

Has been issued since 2014.  
E-ISSN 2413-7243  
2018. 5(2). Issued 2 times a year

## EDITORIAL BOARD

**Bekhterev Viktor** – Sochi State University, Sochi, Russian Federation (Editor in Chief)  
**Belskaya Nataliya** – Ural Federal University, Ekaterinburg, Russian Federation  
**Kuvshinov Gennadiy** – Sochi State University, Sochi, Russian Federation  
**Elyukhin Vyacheslav** – Center of Investigations and Advanced Education, Mexico, Mexico  
**Kestutis Baltakys** – Kaunas University of Technology, Kaunas, Lithuania  
**Mamardashvili Nugzar** – G.A. Krestov Institute of Solution Chemistry of the Russian Academy of Sciences, Ivanovo, Russian Federation  
**Maskaeva Larisa** – Ural Federal University, Ekaterinburg, Russian Federation  
**Md Azree Othuman Mydin** – Universiti Sains Malaysia, Penang, Malaysia  
**Navrotskii Aleksandr** – Volgograd State Technical University, Volgograd, Russian Federation  
**Ojovan Michael** – Imperial College London, London, UK

Journal is indexed by: **CrossRef** (UK), **Electronic scientific library** (Russia), **Journal Index** (USA), **Open Academic Journals Index** (Russia), **ResearchBib** (Japan), **Scientific Indexing Services** (USA)

All manuscripts are peer reviewed by experts in the respective field. Authors of the manuscripts bear responsibility for their content, credibility and reliability.

Editorial board doesn't expect the manuscripts' authors to always agree with its opinion

Postal Address: 1367/4, Stara Vajnorska str., Bratislava – Nove Mesto, Slovakia, 831 04  
Release date 15.09.18.  
Format 21 × 29,7/4.

Website: <http://ejournal14.com/en/index.html> Headset Georgia.  
E-mail: [evr2010@rambler.ru](mailto:evr2010@rambler.ru)

Founder and Editor: Academic Publishing House Researcher s.r.o. Order № 113.

**European Reviews of Chemical Research**

2018

Is. **2**

C O N T E N T S

**Articles and Statements**

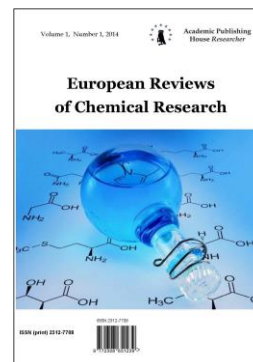
A Quantum Chemical Topological Analysis of the C-O Bond Formation in the 32CA Reaction Involving Zwitterionic Specie Type A. Benallou, Z. Lakbaibi, H. El Alaoui El Abdallaoui, H. Garmes .....	42
Theoretical Elucidation of the Mechanism and Regio-Stereoselectivity of the Cycloaddition between Nitrene Ylides and Electron-Deficient Methacrylonitrile A. Benallou, H. El Alaoui El Abdallaoui, H. Garmes .....	51
DFT Study of the Mechanism, Regio- and Stereoselectivity of the Epoxidation Reaction of the Methyl 2-((2R,4aR)-4a,8-dimethyl-1,2,3,4,4a,5,6,7-octahydro Naphthalen-2-yl)acrylate by m-CPBA M. El Idrissi, A. El Haib, Y. Hakmaoui, M. Zoubir, M. El Ghoulani, S. Mouatarif, N. Ourhriss, R. El Ajlaoui .....	59
Impact Studies of Pest Control Products used in Closed Production Environments on Food Production Quality by SPME coupled to GC-MS A. Lakhili, M. Fekhaoui, A. Bellaouchou, L. Tahri, A. E. Abidi, M. El idrissi .....	67
Synthesis and Visible Spectra Studies of Novel Pyrazolo/Oxazole Merocyanine Dyes H.A. Shindy, M.A. El-Maghraby, M.M. Goma, N.A. Harb .....	75

Copyright © 2018 by Academic Publishing House Researcher s.r.o.



Published in the Slovak Republic  
European Reviews of Chemical Research  
Has been issued since 2014.  
E-ISSN: 2413-7243  
2018, 5(2): 42-50

DOI: 10.13187/erchr.2018.2.42  
[www.ejournal14.com](http://www.ejournal14.com)



## Articles and Statements

### A Quantum Chemical Topological Analysis of the C-O Bond Formation in the 3<sub>2</sub>CA Reaction Involving Zwitterionic Specie Type

Abdelilah Benallou <sup>a,\*</sup>, Zouhair Lakbaibi <sup>b</sup>, Habib El Alaoui El Abdallaoui <sup>a</sup>, Hocine Garmes <sup>a</sup>

<sup>a</sup> University Chouaib Doukkali, El Jadida, Morocco

<sup>b</sup> University of Mohammed V, Ibn Batouta Rabat, Morocco

#### Abstract

The mechanism nature of the 3<sub>2</sub>CA reaction involving zwitterionic species has been performed; and thus, the changes of electron density associated with the O-C and C-C bond formation along IRC are characterized. Conceptual DFT analyses of the most favorable adduct, Endo-mode  $\alpha$ ; shows that the electronic flux will takes place from nitron to methacrylonitrile moiety. Furthermore, ELF topological analysis based on the electron density predicts that C-C bond is formed by the coupling of two pseudoradical centers generated at the most significant atoms of the molecules, while O-C bond is formed by the donation of the some electron density given by the lone pair. Two-stage one-step is the most probably mechanism of this reaction, the first stage aims for the formation of C2-C3  $\sigma$  bond while the second stage aims for the formation of O1-C1  $\sigma$  bond. In general, the observed asynchronicity of this 3<sub>2</sub>CA reaction can be related mainly to the asymmetric reorganization of the electron density at the most attractive centers.

**Keywords:** 3<sub>2</sub>CA, DFT, Cycloaddition, ELF, Nitron.

#### 1. Introduction

Organic compounds of small cycles are of great interest in medicinal chemistry (De Luca, 2006), and are swiftly prepared from a [3+2] cycloaddition (3<sub>2</sub>CA) reaction between a Three Atom- Component (TAC) and an ethylene derivative (see Fig. 1). While TACs are species including four electrons delocalized among three continuous atoms. The 3<sub>2</sub>CA reactions have proven to be a powerful synthetic tool in the construction of five-membered heterocyclic compounds (Padwa et al., 2002). Since the introduction of the chemical bond concept has been explored at the beginning of the 20th century by G. N. Lewis (Irvin, 1938), a lot of theoretical models have been developed to understand the structure and chemical reactivity of the subject. Quantum chemical tools based on the valence bond theory, molecular orbital theory, and the most recent density functional theory (DFT) have proven to be useful to improve the study of structure and reactivity (Confalone et al., 1988; Benallou et al., 2016; Benallou et al., 2016; Benallou et al., 2017; Benallou et al., 2016; Benallou et al., 2017). One appealing procedure that provides a more straightforward connection between the electron density distribution and the chemical structure is the quantum chemical

\* Corresponding author

E-mail addresses: [abdo\\_benallou@yahoo.fr](mailto:abdo_benallou@yahoo.fr) (A. Benallou)

topological (QCT) analysis of the electron density based on the electron localization function (ELF) (Brandi et al., 2009; Benallou et al., 2018; Benallou et al., 2018). In this sense, Silvi and Savin presented the ELF in a very chemical manner, using their topological analysis as an appealing model of chemical bonding (Malinina et al., 2014). Moreover, the characterization of the electron density reorganization to evidence the bonding changes along a reaction path is the most attractive method to analyze a reaction mechanism. A number of the Molecular Electron Density Theory (MEDT) (Domingo, 2016) devoted to the study of the reactivity and mechanism of three-atom-components (TACs), however their contribution in the 32CA reactions have permitted establishing a useful classification of this class of cycloaddition reactions, in which associate to the electronic structure and behavior of the TAC into *pseudodiradical*-type (*pr*-type, typically an azomethine ylide), zwitterionic-type (*zw*-type, typically a nitron) reactions (Figure 2) (Domingo, Emamian, 2014). Usually, nitrones are good nucleophiles that react with electron-deficient alkenes (Domingo et al., 2014).

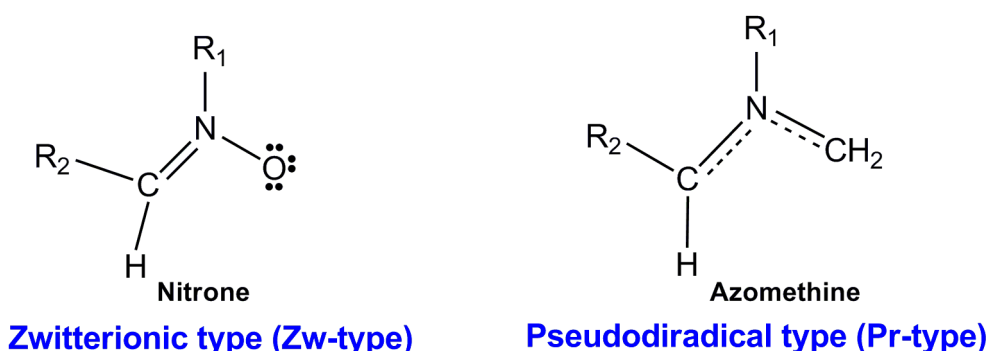


**Fig. 1.** Electronic structure of TACs and the proposed reactivity zwitterionic and pseudodiradical types in 32CA reactions

In this letter, the 32CA reactions of nitron with electronic deficient methacrylonitrile derivative (Carmona et al., 2016), are studied within the MEDT through DFT calculations at the B3LYP/6-31G(d) computational level. This study is dedicated to the most favorable adduct, *endo*  $\alpha$ , the preference of the region-specific *Endo* is confirmed by Parr functions and is strengthened by the thermodynamically evaluation (Figure 2). A quantum chemical topological analysis of the C-C and O-C single bond formation in organic reactions involving cationic species along these 32CA reactions is performed in order to characterize the molecular mechanisms of this cycloaddition reaction.

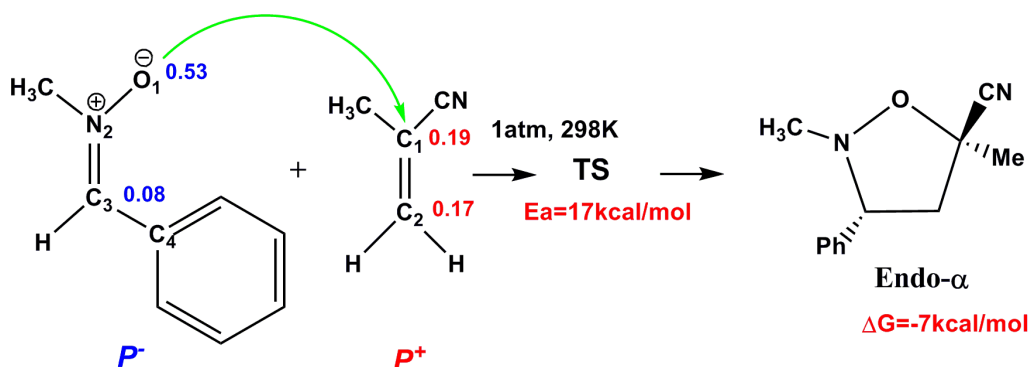


**Fig. 2.** 32CA reaction of nitron (left side) with methacrylonitrile, nucleophilic  $P^-$  and electrophilic  $P^+$  Parr functions

## 2. Computational methods

DFT computations were carried out using the B3LYP exchange–correlation functional (Lee et al., 1988; Becke, 1993), the equilibrium geometries have been optimized at the 6-31G(d) basis set level on Gaussian 09 (Frisch et al., 2009), using Berny's algorithm (Schlegel, 1981). Atomic

electronic populations and reactivity indices were calculated using natural population (NPA). The global electrophilicity index  $\omega$  (Parr et al., 1999), was given by the following expression  $\omega = \mu^2 / \eta$ , in terms of the electronic chemical potential  $\mu = \epsilon_{\text{HOMO}} + \epsilon_{\text{LUMO}} / 2$  and the chemical hardness  $\eta = \epsilon_{\text{LUMO}} - \epsilon_{\text{HOMO}}$ . Both quantities could be approached in terms of the one-electron energies of the frontier molecular orbital HOMO and LUMO, and as and, respectively. The empirical nucleophilicity index  $N$  (Domingo et al., 2011),  $N = (N_{(\text{HOMO-reagent})} - N_{(\text{HOMO-TCE})})$  based on the HOMO energies obtained within the Kohn-Sham (Kohn, Sham, 1965), and defined as the nucleophilicity was referred to tetracyanoethylene (TCE). Electrophilic  $P_k^+$  nucleophilic  $P_k^-$  Parr functions (Domingo et al., 2013) were obtained through analysis of the Mulliken atomic spin density (ASD) of the radical anion and radical cation of the reagents.

The electronic structures of stationary points were analyzed by the natural bond orbital (NBO) method (Reed et al., 1988) and by ELF topological analysis (Savin et al., 1996). The ELF study was performed with the Multiwfn program (Tian, Feiwu, 2012) using the corresponding mono determinantal wave-functions of the selected structures of the IRC.

### 3. Results and discussions

In order to obtain a greater understanding of the bonding formation in the 32CA reaction, the present study has been divided into three parts: (i) in the first one, an analysis of the CDFT reactivity indices at the ground state (GS) of the reagents involved in the 32CA reaction of nitrene with methacrylonitrile is performed; (ii) then, an ELF topological analysis of the electronic structure associated with the 32CA reaction of nitrene and methacrylonitrile are explored and characterized; (iii) in the third part, a topological analysis of the ELF of the nitrene and methacrylonitrile is performed in order to characterize their electronic structures, the C-O bond formation and mechanism nature.

#### 3.1. Analysis of the CDFT reactivity indices of nitrene and methacrylonitrile

An analysis of the CDFT reactivity indices computed in gas phase at the 298K of nitrene with methacrylonitrile was performed to predict their reactivity in 32CA reactions. The global indices, namely, the electronic chemical potential,  $\mu$ , chemical hardness,  $\eta$ , electrophilicity,  $\omega$ , and nucleophilicity,  $N$ , at the ground state (GS) of the reagents involved in these 32CA reactions are given in Table 1.

**Table 1.** B3LYP/6-31G(d) electronic chemical potential ( $\mu$ ), chemical hardness ( $\eta$ ), electrophilicity ( $\omega$ ) and nucleophilicity ( $N$ ), in eV, of nitrene and methacrylonitrile

Reagent	HOMO(au)	LUMO(au)	$\mu$ (eV)	$\eta$ (eV)	$\omega$ (eV)	$N$ (eV)
Nitrene	-0.20231	-0.04651	-2.1	4.2	0.5	3.6
Methacrylonitrile	-0.27715	-0.04511	-3.1	6.3	0.8	1.6

The electronic chemical potential of nitrene  $\mu = -2.1\text{eV}$ , is higher to that of methacrylonitrile,  $\mu = -3.1\text{eV}$ . Thus, the nitrene moiety has a tendency to exchange electron density with methacrylonitrile along this 32CA reaction, so the electro, flow will take place from nitrene to methacrylonitrile. So, methacrylonitrile presents an electrophilicity  $\omega$  index of  $0.8\text{eV}$ , being classified as a feeble electrophile and as a moderate nucleophile,  $1.6\text{eV}$ . At this time, nitrene behaves as a great nucleophile which the nucleophilicity  $N$  index equal  $3.6\text{eV}$  according to the nucleophilicity scales. The electrophilicity of methacrylonitrile is close to that of nitrene  $0.5\text{eV}$ , indicates strongly this reaction is moderately polar. Therefore, in this 32CA reaction, nitrene and methacrylonitrile moieties behave as nucleophile and electrophile, respectively.

#### 3.2. ELF topological analysis of the electronic structure of nitrene and methacrylonitrile

The reactivity of nitrene can be correlated with their electronic structure. Therefore, an ELF topological analysis of the nitrene and methacrylonitrile was performed in order to characterize the electronic structure of this TAC. The representation and attractor positions of ELF valence basins, as well as ELF electron populations, arising from the ELF topological analysis are shown in Figure 3.

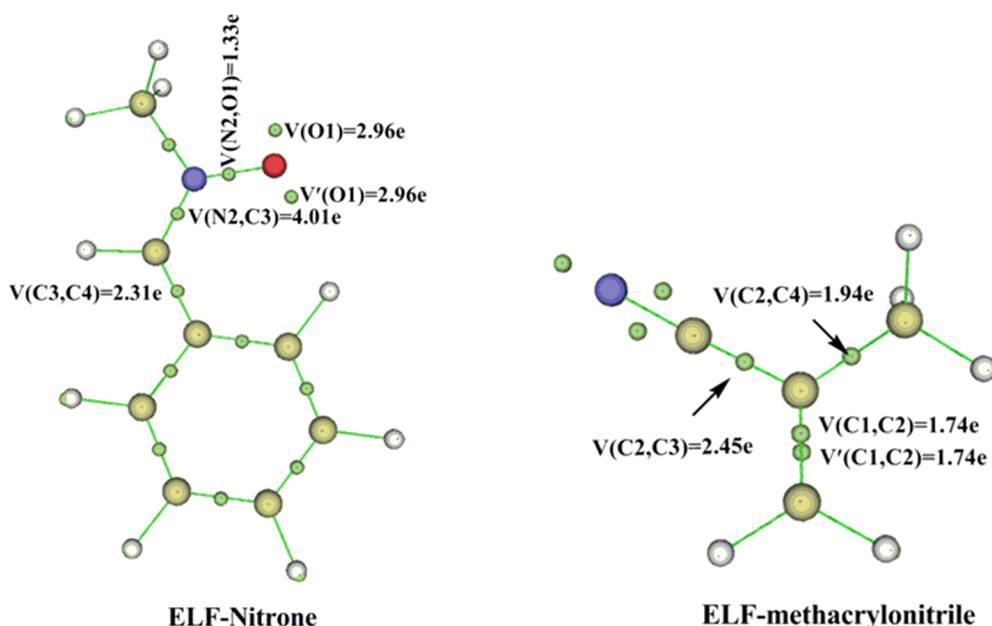


**Fig. 3.** ELF valence basins populations, in e, of nitrone and methacrylonitrile

ELF topology of the nitrone permits establishing the electronic structure distribution on this TAC (see Figure 3). However, nitrone presents two  $V(O1)$  and  $V'(O1)$  monosynaptic basins, integrating 2.96e each one (total  $5.92e \approx 6e$ ), and one  $V(O1,N2)$  disynaptic basin with a population of 1.33e. This behavior suggests that the  $O1-N2$  bonding region is strongly polarized towards the  $O1$  oxygen atom. Additionally, the presence of one  $V(N2,C3)$  disynaptic basin integrating 4.01e indicates that the  $N2-C3$  bonding region has a strong double bond character. Consequently, ELF topology of the nitrone clearly indicates that this TAC is able to participate only in *zw*-type 32CA reactions, as it neither presents a pseudodiradical (Domingo et al., 2010) electronic structure, and thus, ELF topological allows establishing the proposed Lewis structure given in Figure 4. On the other hand, the ELF topology of methacrylonitrile shows the presence of two  $V(C1,C2)$  and  $V'(C1,C2)$  disynaptic basins integrating a total electronic density of 3.48e indicates that the  $C1-C2$  bonding region has a strong double bond character, furthermore  $C2-C3$  and  $C2-C4$  frameworks represent 2.45e and 1.94e respectively, they can be considered single bonds. Consequently, both reagents have the tendency to exchange electron density between them and provide high reactivity.

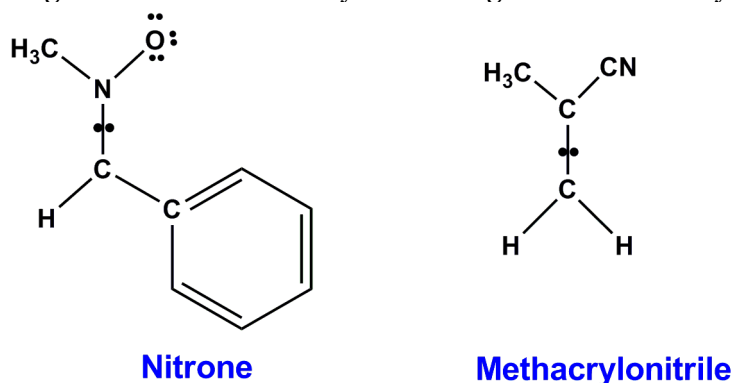


**Fig. 4.** Representation of Lewis structures for nitrone and methacrylonitrile obtained from ELF topological analysis in Zwitterionic specie type

### 3.3. BET/ELF Characterizations of the molecular mechanism of the *zw*-type 32CA reaction between nitrone and methacrylonitrile.

In order to better understanding the bonding changes in organic chemical reactions, the so-called bonding evolution theory (BET) has proved to be a very useful methodological tool (Krokiadis et al., 1997). Several theoretical studies have shown that the topological analysis of the ELF derived

from BET offers a suitable framework for the study of the changes of electron density. This methodological approach is used as a valuable tool to understand the bonding changes along the reaction path, and consequently, to establish the nature of the electronic rearrangement associated with a given molecular mechanism.

In this latter decade, an ELF study of the bonding changes along the zw-type 32CA reactions was carried out in order to understand the bond formation processes and to know the molecular mechanism of this zw-type 32CA process (Ríos-Gutiérrez et al., 2015). An ELF study of the most favorable reaction channel along IRC (Figure 5) associated with the 32CA reaction is performed with the aim of characterizing the molecular mechanism of 32CA reactions involving zwitterionic species. The electronic populations of the most relevant ELF valence basins of selected structures along IRC of this 32CA reaction are listed in Table 2, while the attractor positions for the most relevant points associated with the formation of the O1–C1 and C2–C3 single bonds, are shown in Figure 5.

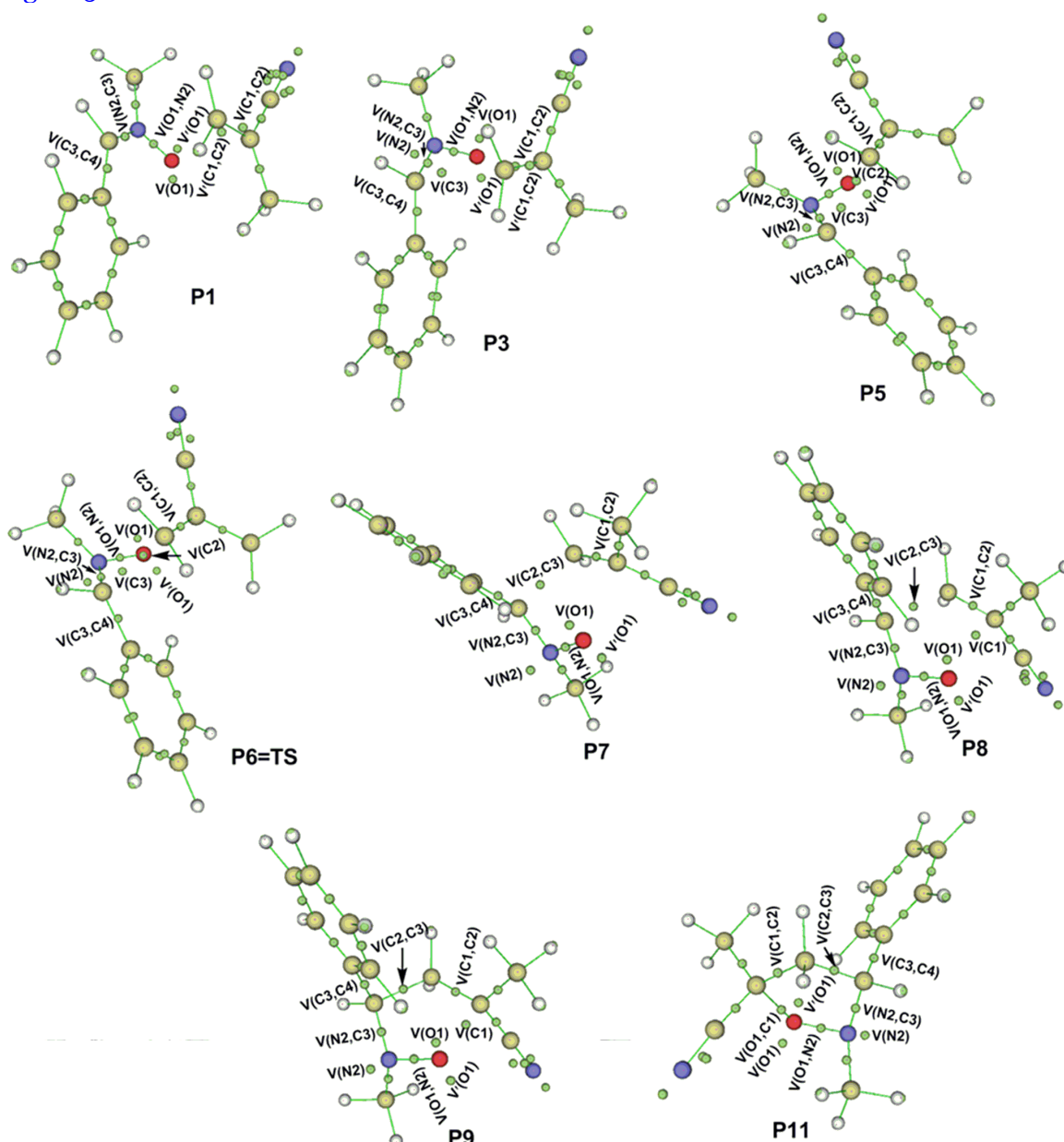


**Fig. 5.** ELF attractors of some selected points of the IRC associated with the formation of the new O–C and C–C single bond in the 32CA reaction of nitron with methacrylonitrile

**Table 2.** Valence basin populations of the most relevant points calculated from the ELF of 32CA reaction of nitron with methacrylonitrile, associated with the O1–C1 and C2–C3 bonds formation step

Points	P1	P2	P3	P4	P5	P6=TS	P7	P8	P9	P10	P11
<b>d(O1-C1)</b>	2.70	2.47	2.37	2.27	2.24	2.21	2.11	2.08	1.91	1.85	1.57
<b>d(C2-C3)</b>	2.81	2.51	2.35	2.19	2.13	2.08	1.92	1.86	1.69	1.66	1.58
<b>V(O1)</b>	2.89	2.89	2.88	2.87	2.86	2.87	2.85	2.86	2.89	2.88	2.67
<b>V'(O1)</b>	3.03	3.00	2.99	2.97	2.95	2.95	2.92	2.92	2.87	2.86	2.73
<b>V(C1)</b>								0.22	0.35	0.35	
<b>V(C2)</b>					0.28	0.39					
<b>V(C3)</b>				0.43	0.49	0.55					
<b>V(N2)</b>			0.86	1.20	1.32	1.41	1.69	1.77	2.02	2.13	2.25
<b>V(O1,C1)</b>											0.87
<b>V(C2,C3)</b>							1.30	1.39	1.65	1.65	1.79
<b>V(O1,N2)</b>	1.31	1.29	1.25	1.21	1.18	1.17	1.13	1.11	1.04	0.97	0.91
<b>V(N2,C3)</b>	3.91	3.94	2.90	2.56	2.45	2.37	2.15	2.09	1.93	1.90	1.88
<b>V(C3,C4)</b>	2.33	2.33	2.32	2.26	2.23	2.20	2.13	2.11	2.06	2.05	2.04
<b>V(C1,C2)</b>	2.30	2.32	3.32	3.28	3.00	2.89	2.67	2.40	2.15	2.07	2.00
<b>V'(C1,C2)</b>	1.70	1.62	3.32	3.28							

Some appealing conclusions can be pointed from this ELF study: the IRC associated with the 32CA reaction of nitron with methacrylonitrile is divided in eleven differentiated points. A behavior that clearly indicates that the bonding changes along this one-step mechanism are non-concerted; the formation of the first C2-C3 single bond takes place at a C-C distance of 1.92Å, by the coupling of the pseudo-diradical of the monosynaptic basin of V(C2) and V(C3) in point P7, with an electronic population of 1.30e. (see Table 2, and the V(C2,C3) disynaptic basin in P7 in Figure 6); in which demand an asymmetric depopulation of the C1-C2 bonding region of methacrylonitrile. At this stage, the second O1-C1 single bond is not yet started. Furthermore this first stage is characterized by the absence of the monosynaptic basin of lone pair V(N2) in P1 and P2 due principally to their contribution to enriching N2-C3 double bond region. The formation of the second O1-C1 single bond takes place at a O-C distance of 1.57Å at the end of the reaction in P11 by the donation of some of the electron density of the O1 oxygen lone pairs to the C1 pseudoradical center of the methacrylonitrile framework (see Table 2, and the V(C1,O1) disynaptic basin in P11 in Figure 6). Note that the O1 oxygen is the most nucleophilic center of nitron and the C1 carbon corresponds to the most electrophilic center of methacrylonitrile. This carbon participates with an appreciable electron density of 0.35e in the formation of the C1-O1 single bond. Subsequently, this 32CA reaction follows a two-stage one-step mechanism in which the formation of the second O1-C1 bond begins when the first C2-C3 single bond is practically already formed. Moreover, the formation of these bonds is totally different and high asynchronous (O-C and C-C bond distances, Table 2); strongly indicates that this reaction is a non-concerted mechanism processes. The depopulation of C1-C2 bonds and the donation of electron density by lone pairs of O1 atom, which revealed by this BET/ELF study can be related to the zwitterionic-type 32CA reaction between nitron and methacrylonitrile. A summarized picture illustrates the bonding changes along the selected points involved in this 32CA reaction is presented in Figure 5, while a representation of the relative position of the selected points along IRC with respect to the energy profile along two-stage one-step mechanism of the 32CA reaction between nitron and methacrylonitrile is given in Figure 7.

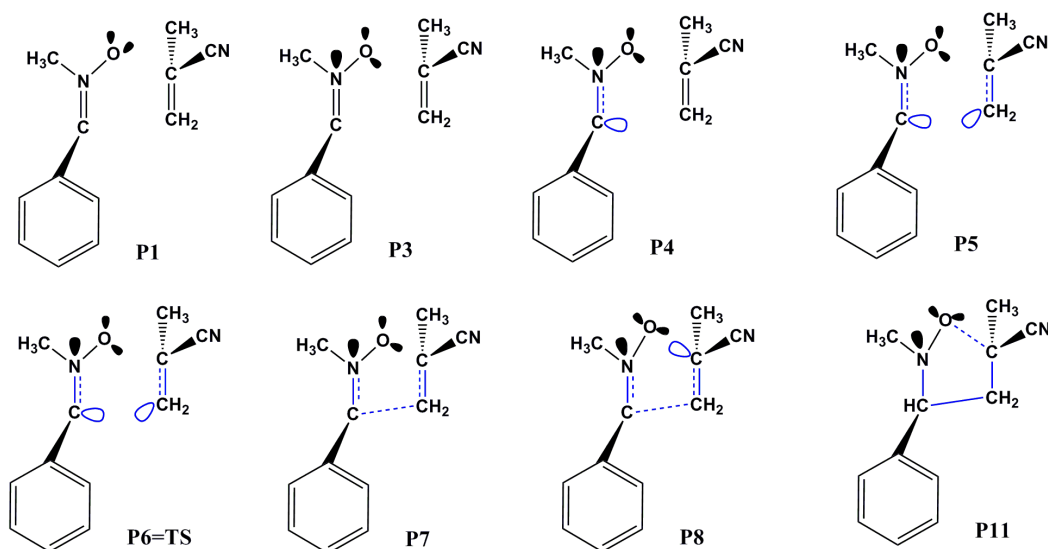


**Fig. 6.** The bonding changes at the selected points involved in the 32CA reaction of nitron with methacrylonitrile

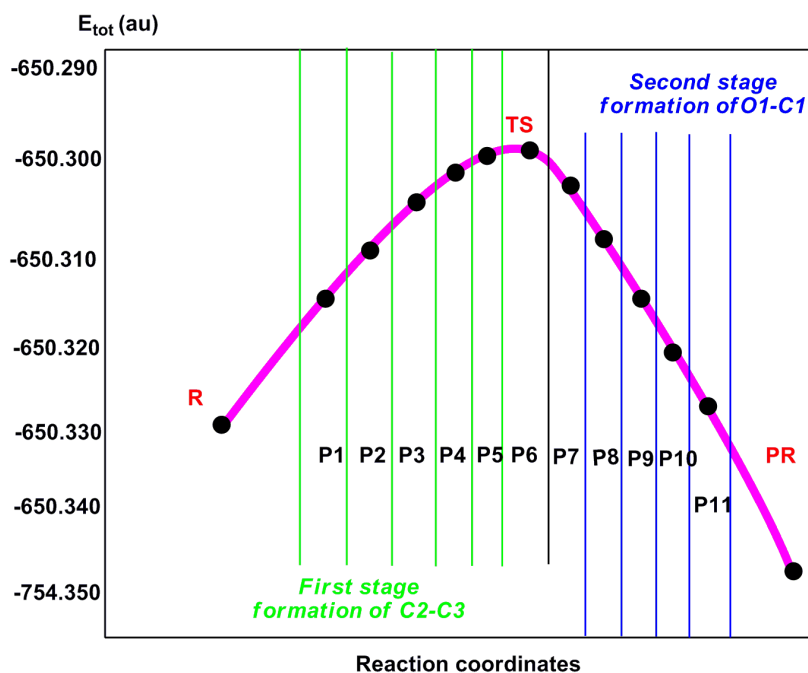


**Fig. 6.** Energy profile, in atomic units (au), along two-stage one-step mechanism associated with the formation of the O1–C1 and C2–C3 single bonds of the 32CA reaction of nitron with methacrylonitrile

#### 4. Conclusion

The 32CA reaction involving zwitterionic species to give small heterocyclic compounds has been studied within MEDT at the DFT B3LYP/6-31G(d) computational level in order to explain the mechanism process and the C–O bonding formation between the rich and the deficient electron atom. The study has been effectuated to the most favorable adduct; the Endo in mode  $\alpha$ . Interestingly, this 32CA reaction can take place along two-stages one-step process; the first stage aims for the formation of the C–C between the weak nucleophilic and electrophilic by coupling of the pseudoradical center as a result of the charge transfer and the depopulation of C–C double bonds. Since, the second stage is located after TS location between the most significant centers to achieve O–C bond in the end of the reaction, by the donation of the some electron density is a part of lone

pair associated with the O atom, which explains that the Zwitterionic character of Nitron moiety. What means that this reaction is not concerted process. So, the asymmetric reorganization of electron density can be responsible of the observed asynchronicity of this reaction.

## References

- De Luca, 2006** – De Luca L. (2006). Naturally occurring and synthetic imidazoles: their chemistry and their biological activities. *Curr. Med. Chem.* 13, 1-23.
- Padwa et al., 2002** – Padwa A., Pearson W.H. (2002). Synthetic applications of 1,3-dipolar cycloaddition chemistry toward heterocycles and natural products; Eds., *John Wiley: Sons*, Vol 59.
- Irvin, 1938** – Irvin, L. (1938). Aliphatic diazo compounds, nitrones, and structurally analogous compounds. systems capable of undergoing 1,3-additions. *Chem. Rev.* 23, 193-285.
- Confalone et al., 1988** – Confalone P. N., Huie E.M. (1988). [3+2] Nitron-olefin cycloaddition reaction. *Org. React. (N.Y.)* 36, 1-174.
- Benallou et al., 2016** – Benallou A., El Alaoui El Abdallaoui H., Garmes H. (2016). Effect of hydrogen bonding on the intramolecular cycloaddition Diels-Alder reaction of triene-amide in an aqueous solution (case of a single molecule of water). *Tetrahedron.* 72, 76-83.
- Benallou et al., 2016** – Benallou A., El Alaoui El Abdallaoui H., Garmes H. (2016). A conceptual DFT approach towards analysing feasibility of the intramolecular cycloaddition Diels-Alder reaction of triene amide in Lewis acid catalyst. *J. Chem. Sci.* 128, 1489-1496.
- Benallou et al., 2017** – Benallou A., Garmes H., El Alaoui E.H. (2017). Understanding the quantitative role of the binding chain (CH<sub>2</sub>)<sub>n</sub> (n=1,2 and 3) on the physicochemical character in the intramolecular reaction: Case of triene-amide. *Mor. J. Chem.* 5, 641-651.
- Benallou et al., 2016** – Benallou A., Garmes H., El Alaoui E.H. (2016). An approached method for predict the nature of the reaction mechanism by assessment of the binding chain (CH<sub>2</sub>)<sub>n</sub> (n=1, 2 and 3) role to the intramolecular cycloaddition Diels-Alder reaction of triene amide. *Mor. J. Chem.* 4, 1021-1028.
- Benallou et al., 2017** – Benallou A., Garmes H., El Alaoui E.H. (2017). Qualitative approach of binding chain (CH<sub>2</sub>)<sub>n</sub> (n=2 to 3) role on the physicochemical character in the intramolecular reaction: case of triene amide molecule. *MAY. J. Chem. Eng.* 1, 1-9.
- Brandi et al., 2009** – Brandi A., Cardona F., Cicchi S., Cordero F.M., Goti A. (2009). Stereocontrolled cyclic nitron cycloaddition strategy for the synthesis of pyrrolizidine and indolizidine alkaloids. *Chem. Eur. J.* 15, 7808-7821.
- Benallou et al., 2018** – Benallou A., El Alaoui E.H., Garmes H. (2018). C-C bond formation in the intramolecular Diels-Alder reaction of triene amides. *Heliyon.* 4, e00504.
- Benallou et al., 2018** – Benallou A., El Alaoui E.H., Garmes H. (2018). An investigation of the reason of not feasibility of hetero-diels-alder reaction of isoselenazole with unsymmetrical acetylenic dienophile: A conceptual DFT study and topological analysis of ELF function. *European Journal of Molecular Biotechnology.* 6(1), 3-15.
- Malinina et al., 2014** – Malinina J., Tran T.Q., Stepanov A.V., Gurzhiy V.V., Starova G.L., Kostikov R.R., Molchanov A.P. (2014). [3+2] Cycloaddition reactions of arylallenes with C-(N-arylcarbonyl)- and C,C-bis(methoxycarbonyl)nitrones and subsequent rearrangements. *Tetrahedron Lett.* 55, 3663-3666.
- Domingo, 2016** – Domingo L.R. (2016). Molecular electron density theory: A modern view of reactivity in organic chemistry. *Molecules.* 21, 1319-1333.
- Domingo, Emamian, 2014** – Domingo L.R., Emamian S.R. (2014). Understanding the mechanisms of [3+2] cycloaddition reactions. The pseudoradical versus the zwitterionic mechanism. *Tetrahedron.* 70, 1267-1273.
- Domingo et al., 2014** – Domingo L.R., Aurell M.J., Pérez P. (2014). A DFT analysis of the participation of zwitterionic TACs in polar [3+2] cycloaddition reactions. *Tetrahedron.* 70, 4519-4525.
- Carmona et al., 2016** – Carmona D., Viguri F., Asenjo A., Lamata P., Lahoz F.J., García-Orduña P. (2016). Asymmetric 1,3-dipolar cycloaddition reactions between methacrylonitrile and nitrones catalysed by well-defined M(diphosphane) (M=Rh, Ir) complexes. *Tetrahedron Asymmetry.* 27, 454-462.

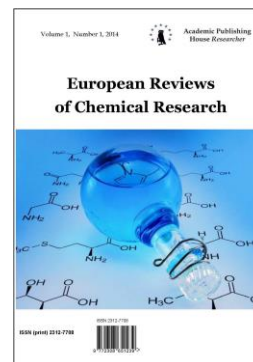
- Lee et al., 1988 – Lee C., Yang W., Parr R.G. (1988). Development of the colle-salvetti correlation-energy formula into a functional of the electron density. *Phys. Rev. B* 37, 785.
- Becke, 1993 – Becke A.D. (1993). Density- functional thermochemistry. III. The role of exact exchange. *J. Chem. Phys.* 98, 5648–5652.
- Frisch et al., 2009 – Frisch M.J. et al. (2009). Gaussian 09, Revision A.02, Gaussian, Inc., Wallingford, CT.
- Schlegel, 1982 – Schlegel H.B. (1982). Optimization of equilibrium geometries and transition structures. *J. Comput. Chem.* 3, 214–218.
- Parr et al., 1999 – Parr R.G., Szentpaly L.V., Liu S. (1999). Electrophilicity Index. *J. Am. Chem. Soc.* 121, 1922–1924.
- Domingo et al., 2011 – Domingo L.R., Pérez P. (2011). The nucleophilicity N index in organic chemistry. *Org. Biomol. Chem.* 9, 7168–9175.
- Kohn, Sham, 1965 – Kohn W, Sham L. (1965). Self-consistent equations including exchange and correlation effects. *J. Phys. Rev.* 140, 1133.
- Domingo et al., 2013 – Domingo L.R., Pérez P., Sáez J.A. (2013). Understanding the local reactivity in polar organic reactions through electrophilic and nucleophilic Parr functions. *RSC Adv.* 3, 1486–1494.
- Reed et al., 1988 – Reed A.E., Curtiss L.A., Weinhold F. (1988). Intermolecular interactions from a natural bond orbital, donor-acceptor viewpoint. *Chem. Rev.* 88, 899.
- Savin et al., 1996 – Savin A., Silvi B., Colonna F. (1996). Topological analysis of the electron localization function applied to delocalized bonds. *Can. J. Chem.* 74, 1088–1096.
- Tian, Feiwu, 2012 – Tian L., Feiwu C. (2012). Multiwfn: A multifunctional Wavefunction analyzer. *J. Comp. Chem.* 33, 580-592.
- Domingo et al., 2010 – Domingo L.R., Chamorro E., Pérez P. (2010). Understanding the high reactivity of the azomethine ylides in [3+2] cycloaddition reactions. *Lett. Org. Chem.* 7, 432–439.
- Krokidis et al., 1997 – Krokidis X., Noury S., Silvi B. (1997). Characterization of elementary chemical processes by catastrophe theory. *J. Phys. Chem. A* 101, 7277–7282.
- Ríos-Gutiérrez et al., 2015 – Ríos-Gutiérrez M., Pérez P., Domingo L.R. (2015). A bonding evolution theory study of the mechanism of [3+2] cycloaddition reactions of nitrones with electron-deficient ethylenes. *RSC Advances.* 5, 58464–58477.

Copyright © 2018 by Academic Publishing House Researcher s.r.o.



Published in the Slovak Republic  
European Reviews of Chemical Research  
Has been issued since 2014.  
E-ISSN: 2413-7243  
2018, 5(2): 51-58

DOI: 10.13187/erchr.2018.2.51  
[www.ejournal14.com](http://www.ejournal14.com)



## Theoretical Elucidation of the Mechanism and Regio-Stereoselectivity of the Cycloaddition between Nitron Ylides and Electron-Deficient Methacrylonitrile

Abdelilah Benallou <sup>a,\*</sup>, Habib El Alaoui El Abdallaoui <sup>a</sup>, Hocine Garmes <sup>a</sup>

<sup>a</sup> University Chouaib Doukkali, El Jadida, Morocco

### Abstract

The [3+2] cycloaddition (32CA) reaction of nitron with methacrylonitrile, has been studied within Electron localization function (ELF) at the DFT B<sub>3</sub>LYP/6-31G(d) computational level. This feeble-polar 32CA reaction, which takes place via an asynchronous mechanism, proceeds with a moderate activation energy of 17 kcal/mol, for the most favourable adduct; endo- $\alpha$ , and presents low stereo- and regioselectivities due to the existence of various competitive channels (exo( $\alpha,\beta$ ) and endo( $\alpha,\beta$ )). The Conceptual DFT is in good consistency with the thermodynamically results. ELF analysis shows that 1,3 dipolarophile O1 and C3 atom of nitron are extensively higher in reactivity.

**Keywords:** Nitron; 32Cycloaddition; ELF; DFT; Regio-stereoselectivity.

### 1. Introduction

The first examples of 1,3 dipolar cycloaddition is gathered by Irvin in 1938 (Irvin, 1938), demonstrating that nitrones are capable of undergoing 1,3-additions, the [3+2] cycloaddition (32CA) reaction of nitrones with alkenes (Confalone, Huie, 1988) has been widely used as a key step for the synthesis of heterocycles and natural products (Martin, Jones, 2002). The ready availability and ease of use of nitrones (Merino, 2010), the tendency of the reaction by using chiral Lewis acids (Kanemasa et al., 2002) and the high efficiency of this transformation (Rück-Braun et al., 2005) combine to make this reaction a powerful method for heterocyclic synthesis (Brandi et al., 1997). The asymmetric 1,3-dipolar cycloaddition reactions provide efficient and reliable access to enantiomerically enriched five membered heterocyclic systems (Hassana, Müller, 2015). In particular, the 1,3-dipolar cycloaddition of nitrones to electron-deficient alkenes or alkynes afford one powerful method for the construction of highly substituted isoxazolidine rings (Sibi et al., 2003), which is usually the core framework of many biologically active compounds and readily converted into b- or g-amino alcohols and others. The greatest challenge for the dipolar cycloaddition reactions of nitrones with alkenes (methacrylonitrile) is to control the region and stereoselectivity of the 32CA reactions.

In latest years, computational chemistry has become a principal instrument for chemists and a well-accepted instrument for experimental chemistry. Herein, in order to understand the molecular mechanism and the region-streoselectivity of the 32CA reaction between nitron and electron-deficient methacrylonitrile (Figure 1), a theoretical characterization of the molecular mechanism of this reaction is carried out within the computational methods. We examine analyses of the reactivity indices of the reagents, Parr and Fukui functions are performed and also ELF

\* Corresponding author

E-mail addresses: [abdo\\_benallou@yahoo.fr](mailto:abdo_benallou@yahoo.fr). (A. Benallou)

analysis using density functional theory (DFT) methods with 6-31G(d) basis set. Our aim is to explicate the mechanism and stereo-regioselectivity of such reaction (Figure 1).

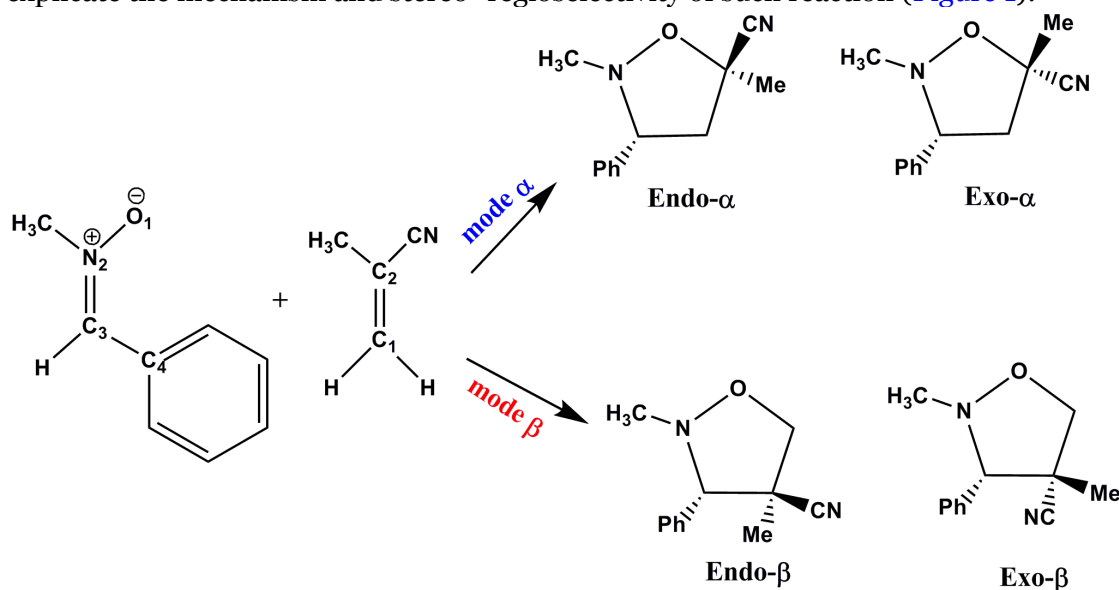


**Fig. 1.** Stereo-regioselectivity of the 32CA reaction of nitron with methacrylonitrile

## 2. Computational methods

DFT computations were carried out using the B3LYP exchange–correlation functional (Lee et al., 1988; Becke, 1993), the equilibrium geometries have been optimized at the 6-31G(d) basis set level on Gaussian 09 (Frisch et al., 2009), using Berny's algorithm (Schlegel, 1982). Atomic electronic populations and reactivity indices were calculated using natural population (NPA). The global electrophilicity index  $\omega$  (Parr et al., 1999) was given by the following expression,  $\omega = \mu^2 / \eta$ , in terms of the electronic chemical potential  $\mu = \epsilon_{\text{HOMO}} + \epsilon_{\text{LUMO}} / 2$  and the chemical hardness  $\eta = \epsilon_{\text{LUMO}} - \epsilon_{\text{HOMO}}$ . Both quantities could be approached in terms of the one-electron energies of the frontier molecular orbital HOMO and LUMO, and as and, respectively. The empirical nucleophilicity index  $N$  (Domingo, Pérez, 2011)  $N = (N_{(\text{HOMO-reagent})} - N_{(\text{HOMO-TCE})})$  based on the HOMO energies obtained within the Kohn-Sham (Kohn, Sham, 1965), and defined as the nucleophilicity was referred to tetracyanoethylene (TCE). Electrophilic  $P_k^+$  and nucleophilic  $P_k^-$  Parr functions were obtained through analysis of the Mulliken atomic spin density (ASD) of the radical anion and radical cation of the reagents. The condensed form of the functions of Fukui in a molecule with  $N$  electrons was proposed (Chattaraj et al., 2012; Benallou et al., 2016; Benallou et al., 2016):

$$f_k^+ = [q_k(N+1) - q_k(N)] \text{ for nucleophilic attack}$$

$$f_k^- = [q_k(N) - q_k(N-1)] \text{ for electrophilic attack}$$

$q_k(N)$ : Electronic population of the atom  $k$  in the neutral molecule.

$q_k(N+1)$ : Electronic population of the atom  $k$  in the anionic molecule.

$q_k(N-1)$ : Electronic population of the atom  $k$  in the cationic molecule.

The electronic structures of stationary points were analyzed by the natural bond orbital (NBO) method (Reed et al., 1988) and by ELF topological analysis (Savin et al., 1996; Benallou et al., 2018; Benallou et al., 2018; Benallou, 2018). The ELF study was performed with the Multiwfn program (Tian, Feiwu, 2012) using the corresponding mono determinantal wave-functions of the selected structures of the IRC.

## 3. Results

In order to obtain a greater understanding of the 32CA reaction, the present study has been divided into four parts: (i) in the first one, an analysis of the CDFT reactivity indices at the ground state (GS) of the reagents involved in the 32CA reactions of nitron with methacrylonitrile is performed; (ii) then, the reaction paths associated the 32CA reaction of nitron with methacrylonitrile are explored and characterized; (iii) in the third part, a topological analysis of the ELF of the simplest allene and methacrylonitrile is performed in order to characterize their

electronic structures. Finally, a characterization of the reaction paths associated with the 32CA reaction of nitron and methacrylonitrile is carried out.

### 3.1. Analysis of the CDFT reactivity indices of nitron and methacrylonitrile

An analysis of the CDFT reactivity indices computed in gas phase at the 298K of nitron with methacrylonitrile was performed to predict their reactivity in 32CA reactions. The global indices, namely, the electronic chemical potential,  $\mu$ , chemical hardness,  $\eta$ , electrophilicity,  $\omega$ , and nucleophilicity,  $N$ , at the ground state (GS) of the reagents involved in these 32CA reactions are given in Table 1.

**Table 1.** B3LYP/6-31G(d) electronic chemical potential ( $\mu$ ), chemical hardness ( $\eta$ ), electrophilicity ( $\omega$ ) and nucleophilicity ( $N$ ), in eV, of nitron and methacrylonitrile

Reagent	HOMO	LUMO	$\mu$ (eV)	$\eta$ (eV)	$\omega$ (eV)	$N$ (eV)
Nitron	-0.20231	-0.04651	-2.1	4.2	0.5	3.6
Methacrylonitrile	-0.27715	-0.04511	-3.1	6.3	0.8	1.6

The electronic chemical potential of nitron  $\mu=-2.1\text{eV}$ , is practically higher to that of methacrylonitrile,  $\mu=-3.1\text{eV}$ . Thus, the nitron moiety has a tendency to exchange electron density with methacrylonitrile along this 32CA reaction, so the electro, flow will take place from nitron to methacrylonitrile. Methacrylonitrile presents an electrophilicity  $\omega$  index of  $0.8\text{eV}$ , being classified as a feeble electrophile and as a moderate nucleophile,  $1.6\text{eV}$ . At this time, nitron behaves as a great nucleophile which presents a nucleophilicity  $N$  index about  $3.6\text{eV}$  according to the nucleophilicity scales. The electrophilicity of methacrylonitrile is close to that of nitron  $0.5\text{eV}$ , indicates strongly this reaction is moderately polar. Therefore, at this 32CA reaction, Nitron and methacrylonitrile moieties behaves as nucleophile and electrophile, respectively.

### 3.2. An analysis of the reactivity by estimating the local indices of the reagents

By approaching a non-symmetric electrophilic/nucleophilic pair along an organic reaction process, the most favourable reactive channel is that associated with the initial two-center interaction between the most electrophilic center of the electrophile and the most nucleophilic center of the nucleophile. Recently, Domingo proposed the nucleophilic  $P_k^-$  and  $P_k^+$  electrophilic Parr functions, derived from the changes of spin electron-density. Accordingly, the nucleophilic and electrophilic Parr functions centers and Fukui indices of the reagents involved in this 32CA reaction are portrayed in Figure 2.

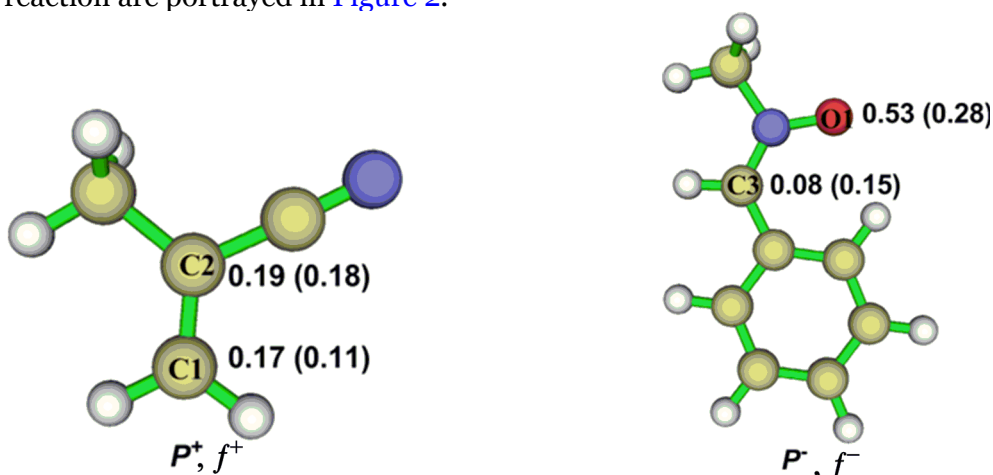


**Fig. 2.** The nucleophilic  $P_k^-$  and electrophilic  $P_k^+$  Parr functions and Fukui indices (in parentheses)

It is worth mentioning that the most favourable electrophile–nucleophile interaction along the 32CA reaction between nitron (right side) and methacrylonitrile in moderate polar process will take place between the most nucleophilic center of nitron, the O1 oxygen atom, and the most

electrophilic center of methacrylonitrile, the C2 carbon atom. In which the greater value of nucleophilic and electrophilic Parr and Fukui functions are attributed consecutively to the O1 and C1 atoms, respectively (Figure 2), and then, O1 atom is very rich electronically, it has considered as an electron donor. So,  $\alpha$ - mode is eventually the most favourable pattern channel in this 32CA reaction.

### 3.3. ELF analysis of electron density involved at the centers reactive associated with 32CA reaction

One appealing procedure that provides a straightforward connection between the electron density distribution and the chemical structure is the quantum chemical analysis of the Becke and Edgecombe's Electron Localization Function (ELF). An ELF topological analysis of the electronic structure of nitron and methacrylonitrile make it possible to explain the reactivity of these reagents. The ELF of nitron shows the presence of two monosynaptic basins,  $V(O1)$  and  $V'(O1)$ , associated with the lone pairs integrating 2.96e each one (see Fig. 3). This electronic characteristic of nitron allowed associating its reactivity to that of a high reactive pseudo-diradical species. While methacrylonitrile presents two disynaptic basins,  $V(C1,C2)$  and  $V'(C1,C2)$ , associated with double bonds of C1-C2, integrating 1.74e each one. So, Nitron represents high reactivity by their electron density established in O1 atom, allowing high performance with both centers reactive of methacrylonitrile, C1 and C2 atom.

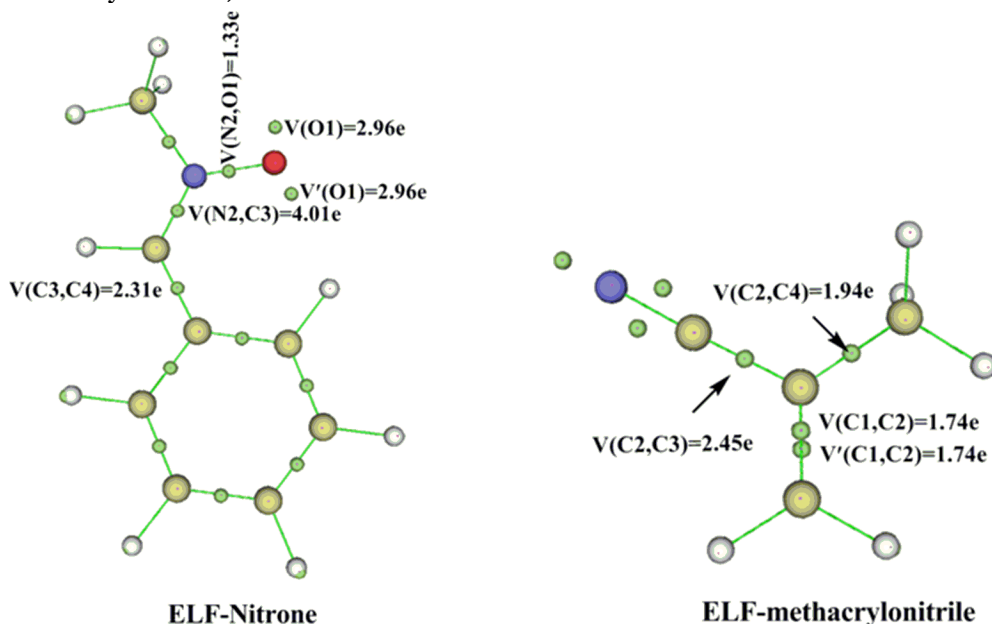


**Fig. 3.** Some significant valence ELF basins of Nitron and Methacrylonitrile. The non-bonding  $V(M)$  and bonding  $V(M,N)$  monosynaptic basins are represented in green circle

### 3.4. Study of the reaction paths associated with the 32CA reaction of nitron and methacrylonitrile

Due to the non-symmetry of the two reagents, the (3+2) cycloaddition reaction of nitron with methacrylonitrile can take place along four isomeric channels: one pair of stereoisomeric exo channels of both mode and one pair of regioisomeric endo channels of both  $\alpha$  and  $\beta$  mode (Figure 4). In this part we want to study the stereoselectivity and regioselectivity through evaluating the barrier activation.

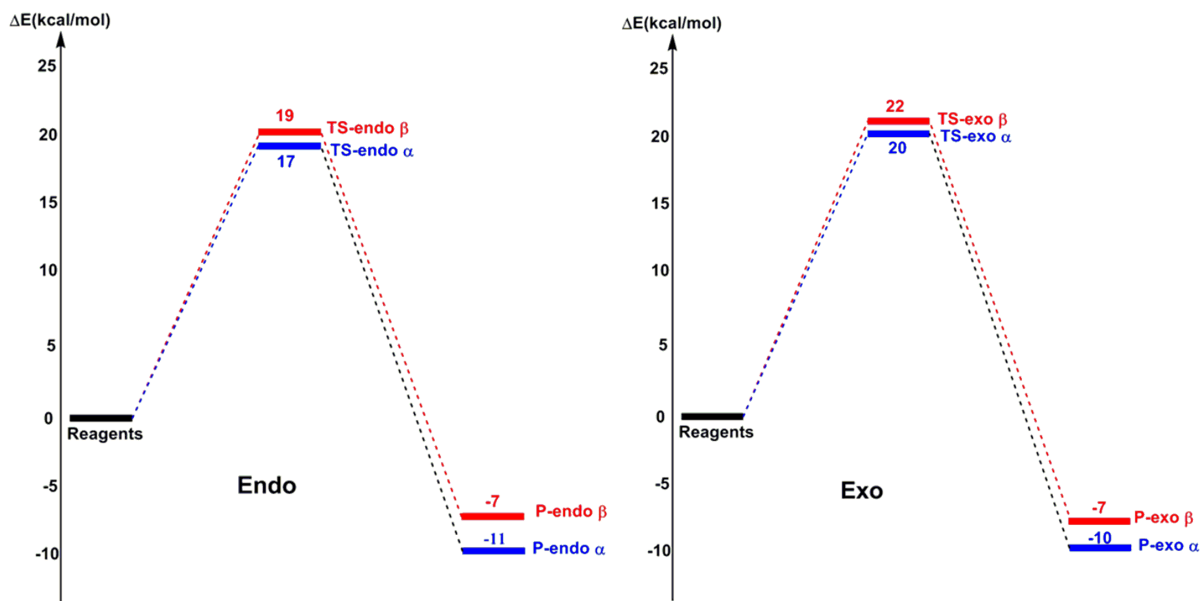


**Fig. 4.** The competitive reactive channels associated with the  $32\text{CA}$  reaction of nitrene with methacrylonitrile. B3LYP/6-31G(d) relative energies, are given in kcal/mol.

The activation energies associated with the competitive channels are 17 (TS-endo  $\alpha$ ), 19 (TS-endo  $\beta$ ), 20 (TS-exo  $\alpha$ ), 22 (TS-exo  $\beta$ ), kcal mol<sup>-1</sup>. So, Endo, in  $\alpha$  mode is the most favourable competitive channel of this reaction. Some appealing conclusions can be drawn from these relative energies: the activation energy associated with the  $32\text{CA}$  reaction via TS-endo  $\alpha$  is 17 kcal mol<sup>-1</sup> lower in energy than remaining regio-specific channels (TS-endo  $\beta$ ), (TS-exo  $\alpha$ ) and (TS-exo  $\beta$ ), indicating that the formation of the product P-endo  $\alpha$  is kinetically very favored.

These  $32\text{CA}$  reactions are exergonic by -7.2, -2.7, -6.5 and -3.2 kcal mol<sup>-1</sup> for P-endo  $\alpha$ , P-endo  $\beta$ , P-exo  $\alpha$  and P-exo  $\beta$ , respectively. Note that the most favourable reactive channel associated with the  $32\text{CA}$  reaction involving is extremely exergonic, the formation of the product P-endo in mode  $\alpha$  is enormously exothermic by -13 kcal mol<sup>-1</sup> to compare with other product, and therefore this channel process is completely irreversible. Consequently, the product P-endo- $\alpha$  is kinetically and thermodynamically favored.

Optimized TSS involved in the  $32\text{CA}$  reactions between nitrene and methacrylonitrile, including some selected distances, are given in [Figure 5](#).

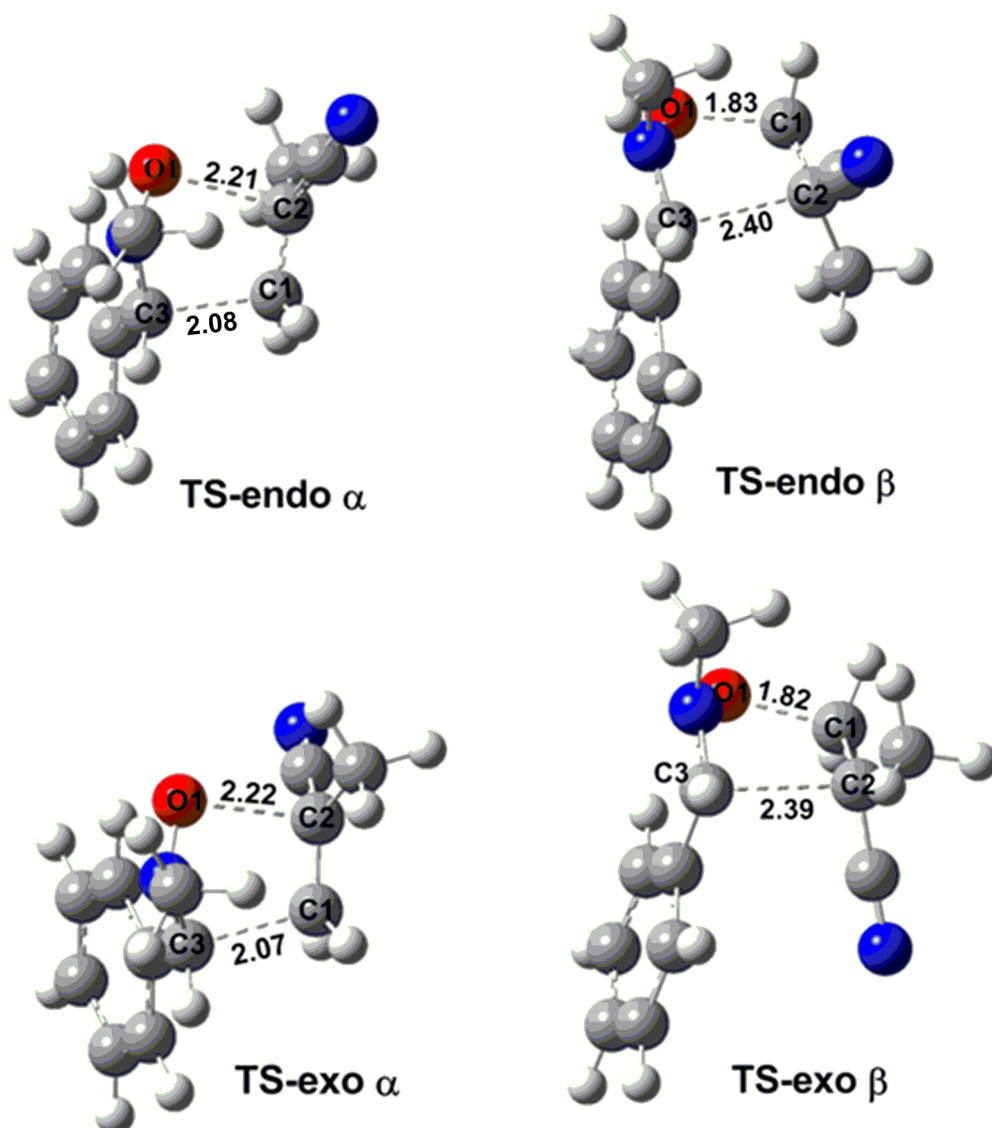


**Fig.5.** B3LYP/6-31G(d) optimized geometries of the TSs involved in the  $32CA$  reactions between nitrene and methacrylonitrile. Distances are given in Angstroms

At the TSs associated with the  $32CA$  reaction, the distances between the atoms involved in the formation of the C–C and C–O single bonds for both region-stereoselective channels are: 2.21Å, 2.22Å (C2–O1) and 2.08, 2.07Å (C1–C3) at TS-endo,exo  $\alpha$  respectively, equally 1.83, 1.82Å (C1–O1) and 2.40 , 2.39Å (C2–C3) at TS-endo,exo  $\beta$ , respectively.

In  $\alpha$ -mode, C1–C3 will be eventually formed first, while in  $\beta$ -mode, O1–C1 bond is formed before C2–C3, regarding the shortest distances involved in these bonds. Therefore, this mechanism process is an asynchronous. In which the integrated C1 atom bonding will be formed early. Consequently, the products Endo, in both  $\alpha$  and  $\beta$  mode are favored.

#### 4. Conclusion

In order to understand the mechanism and regio- and stereospecificity, this reaction has been theoretically studied using DFT methods at the B3LYP/6–31G(d) level of theory. The reactive channels corresponded to the regioselective and stereoselective approach modes have been explored and characterized. We can summarize the results of the present study in the following points:

Analysis of the computed Parr and Fukui functions of the nucleophilic and electrophilic centers between nitrene and methacrylonitrile, as well as thermodynamic calculations at gas phase justifying the preference region- and stereo-selective of Endo in both  $\alpha$  and  $\beta$  mode.

The relatively moderate activation energies found for both modes of this reaction and the high electron density revealed by ELF topological are explained by the high nucleophilic nature of O1 centers atom of nitron, and the moderate electrophilic nature of C1 and C2 atom of methacrylonitriles, giving a good explanation of the activation barrier.

### Reference

- [Irvin, 1938](#) – *Irvin, L.* (1938). Aliphatic diazo compounds, nitrones, and structurally analogous compounds. systems capable of undergoing 1,3-additions. *Chem. Rev.* 23, 193-285.
- [Confalone, Huie, 1988](#) – *Confalone P.N., Huie E.M.* (1988). [3+2] Nitron-olefin cycloaddition reaction. *Org. React. (N.Y.)* 36, 1-174.
- [Martin et al., 2002](#) – *Martin J. N., Jones R. C. F., Padwa A., Pearson W.H.* (2002). In *Synthetic Applications of 1,3-Dipolar Cycloaddition Chemistry toward Heterocycles and Natural Products*, Eds.; Wiley: Chichester, United Kingdom. 59, 1-81.
- [Merino, 2011](#) – *Merino P.* (2011). In *Science of Synthesis*; E. Schaumann, Ed.; George Thieme: Stuttgart. 4, 325-403.
- [Kanemasa et al., 2002](#) – *Kanemasa S., Padwa A., Pearson W.H.* (2002), In *Synthetic Applications of 1,3-Dipolar Cycloaddition Chemistry toward Heterocycles and Natural Products*; Eds.; Wiley: Chichester, United Kingdom. 59, 755.
- [Rück-Braun et al., 2005](#) – *Rück-Braun K., Freysoldt T.H.E., Wierschem F.* (2005). 1,3-Dipolar cycloaddition on solid supports: nitron approach towards isoxazolidines and isoxazolines and subsequent transformations. *Chem. Soc. Rev.* 34, 507-516.
- [Brandi et al., 2009](#) – *Brandi A., Cardona F., Cicchi S., Cordero F.M., Goti A.* (2009). Stereocontrolled cyclic nitron cycloaddition strategy for the synthesis of pyrrolizidine and indolizidine alkaloids. *Chem. Eur. J.* 15, 7808-7821.
- [Hassana, Müller, 2015](#) – *Hassana S., Müller T.J.J.* (2015). Multicomponent Syntheses based upon Copper- Catalyzed Alkyne- Azide Cycloaddition. *Adv. Synth. Catal.* 357, 617-666.
- [Sibi et al., 2003](#) – *Sibi M.P., Prabakaran N., Ghorpade S.G., Jasperse C.P.* (2003). Enantioselective Synthesis of  $\alpha,\beta$ -Disubstituted- $\beta$ -amino Acids. *J. Am. Chem. Soc.* 125, 11796-11797.
- [Lee et al., 1988](#) – *Lee C., Yang W., Parr R.G.* (1988). Development of the colle-salvetti correlation-energy formula into a functional of the electron density. *Phys. Rev. B* 37, 785.
- [Becke, 1993](#) – *Becke A.D.* (1993). Density- functional thermochemistry. III. The role of exact exchange. *J. Chem. Phys.* 98, 5648-5652.
- [Frisch et al., 2009](#) – *Frisch M.J. et al.* (2009). Gaussian 09, Revision A.02, Gaussian, Inc., Wallingford, CT.
- [Schlegel, 1982](#) – *Schlegel H.B.* (1982). Optimization of equilibrium geometries and transition structures. *J. Comput. Chem.* 3, 214-218.
- [Parr et al., 1999](#) – *Parr R.G., Szentpaly L.V., Liu S.* (1999). Electrophilicity Index. *J. Am. Chem. Soc.* 121, 1922-1924.
- [Domingo, Pérez, 2011](#) – *Domingo L.R., Pérez P.* (2011). The nucleophilicity N index in organic chemistry. *Org. Biomol. Chem.* 9, 7168-9175.
- [Kohn, Sham, 1965](#) – *Kohn W, Sham L.* (1965). Self-consistent equations including exchange and correlation effects. *J. Phys. Rev.* 140, 1133.
- [Chattaraj et al., 2012](#) – *Chattaraj P.K., Duley S., Domingo L.R.* (2012). Understanding local electrophilicity/nucleophilicity activation through a single reactivity difference index. *Org. Biomol. Chem.* 10, 2855-2861.
- [Benallou et al., 2016](#) – *Benallou A., El Alaoui El Abdallaoui H., Garmes H.* (2016). Effect of hydrogen bonding on the intramolecular cycloaddition Diels-Alder reaction of triene-amide in an aqueous solution (case of a single molecule of water). *Tetrahedron.* 72, 76-83.
- [Benallou et al., 2016](#) – *Benallou A., El Alaoui El Abdallaoui H., Garmes H.* (2016). A conceptual DFT approach towards analysing feasibility of the intramolecular cycloaddition Diels-Alder reaction of triene amide in Lewis acid catalyst. *J. Chem. Sci.* 128, 1489-1496.
- [Reed et al., 1988](#) – *Reed A.E., Curtiss L.A., Weinhold F.* (1988). Intermolecular interactions from a natural bond orbital, donor-acceptor viewpoint. *Chem. Rev.* 88, 899.

[Savin et al., 1996](#) – *Savin A., Silvi B., Colonna F.* (1996). Topological analysis of the electron localization function applied to delocalized bonds. *Can. J. Chem.* 74, 1088–1096.

[Benallou et al., 2018](#) – *Benallou A., El Alaoui E.H., Garmes H.* (2018). C-C bond formation in the intramolecular Diels-Alder reaction of triene amides. *Heliyon.* 4, e00504.

[Benallou et al., 2018](#) – *Benallou A., El Alaoui E.H., Garmes H.* (2018). The Contribution to Bonding by Lone Pairs in the Hydrogen Transfer of Adenine Tautomerization (3H→9H) in the First Excited Electronic State: ELF Analysis. *European Journal of Molecular Biotechnology.* 6, 16-24.

[Benallou, 2018](#) – *Benallou A.* (2018). An investigation of molecular mechanism and the role of Te-bridged-atom in the formation of polysubstituted pyridines via Hetero-Diels–Alder reaction of isotellurazole with acetylenic dienophile: a molecular electron density study. *J. Chem. Sci.* 130, 102.

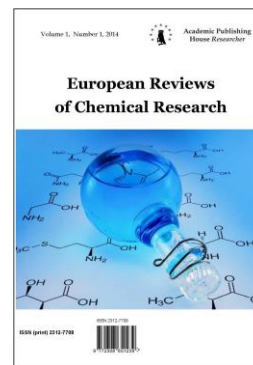
[Tian, Feiwu, 2012](#) – *Tian L., Feiwu C.* (2012). Multiwfn: A multifunctional Wavefunction analyzer. *J. Comp. Chem.* 33, 580-592.

Copyright © 2018 by Academic Publishing House Researcher s.r.o.



Published in the Slovak Republic  
European Reviews of Chemical Research  
Has been issued since 2014.  
E-ISSN: 2413-7243  
2018, 5(2): 59-66

DOI: 10.13187/erchr.2018.2.59  
[www.ejournal14.com](http://www.ejournal14.com)



## DFT Study of the Mechanism, Regio- and Stereoselectivity of the Epoxidation Reaction of the Methyl 2-((2R,4aR)-4a,8-dimethyl-1,2,3,4,4a,5,6,7-octahydro Naphthalen-2-yl)acrylate by m-CPBA

M. El Idrissi <sup>a,\*</sup>, A. El Haib <sup>b</sup>, Y. Hakmaoui <sup>b</sup>, M. Zoubir <sup>a</sup>, M. El Ghoulani <sup>b</sup>, S. Mouatarif <sup>a</sup>, N. Ourhriss <sup>a</sup>, R. El Ajlaoui <sup>b</sup>

<sup>a</sup> Chouaïb Doukkali University, El Jadida, Morocco

<sup>b</sup> Sultan Moulay Slimane University, Beni Mellal, Morocco

### Abstract

The mechanism and regioselectivity of the epoxidation reaction of the methyl 2-((2R,4aR)-4a,8-dimethyl-1,2,3,4,4a,5,6,7-octahydronaphthalen-2-yl)acrylate **1** by m-CPBA, have been theoretically studied at the DFT/ B3LYP/6-31(d) computational level. The possible 1/2/3 regioselective and stereoselective channels were explored and characterized, the energies analysis associated with the different reaction pathways indicates that this epoxidation reaction is highly regioselective, in good conformity with the experimental observations.

**Keywords:** Molecular Electron Density Theory, stereoselective, regioselective, epoxidation, DFT/ B3LYP/6-31(d).

### 1. Introduction

Eudesmane products are pervasive in species of plant (Fraga, 2007). Among them, eudesmane acids and esters have attracted considerable interest due to their extensive spectrum of pharmacological properties: as, isocostic acid (Figure 1), (Zaki et al., 2017) Showing significant antifungal, antibacterial properties (Shtacher, Kashman 1970). The eudesmane acid derivatives have antipyretic properties and the hydrocostic acid is toxic to Artemisia Salina and has an anti-appetizing activity against Spodopetra Littoralis (Barbetti et al., 1985).

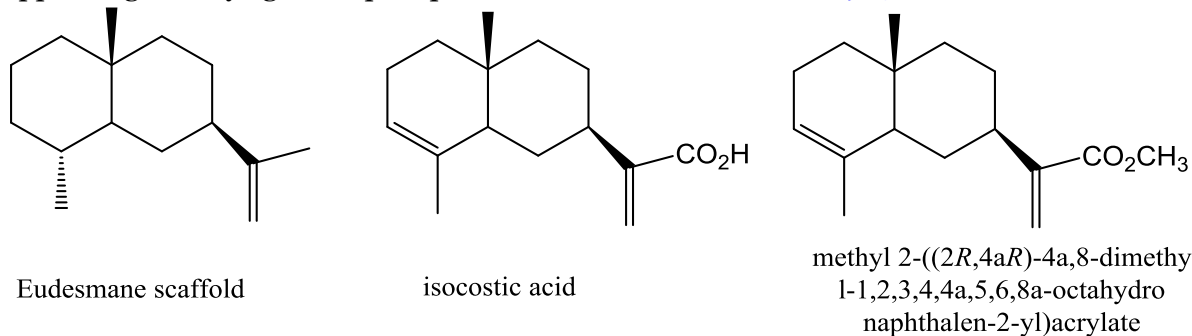


**Fig. 1.** Structures of the eudesmane, isocostic acid and isocostic-methyl ester

\* Corresponding author

E-mail addresses: [idrissi\\_82@hotmail.fr](mailto:idrissi_82@hotmail.fr) (M. El idrissi)

Herein, in order to understand the molecular mechanism, regio- and stereoselectivity of the epoxidation reaction of the methyl 2-((2R,4aR)-4a,8-dimethyl-1,2,3,4,4a,5,6,7-octahydronaphthalen-2-yl)acrylate by m-CPBA (Figure 2), a theoretical characterization of the molecular mechanism of this epoxidation reactions is carried out within the MEDT using DFT methods at the B3LYP/6-31G(d) computational level, this new theory very recently proposed by Domingo to study the reactivity in organic chemistry named Molecular Electron Density Theory (MEDT) (Domingo et al 2016), when the partition of the total density of the TS geometry into two separated structure does not any physical sense within density functional DFT.

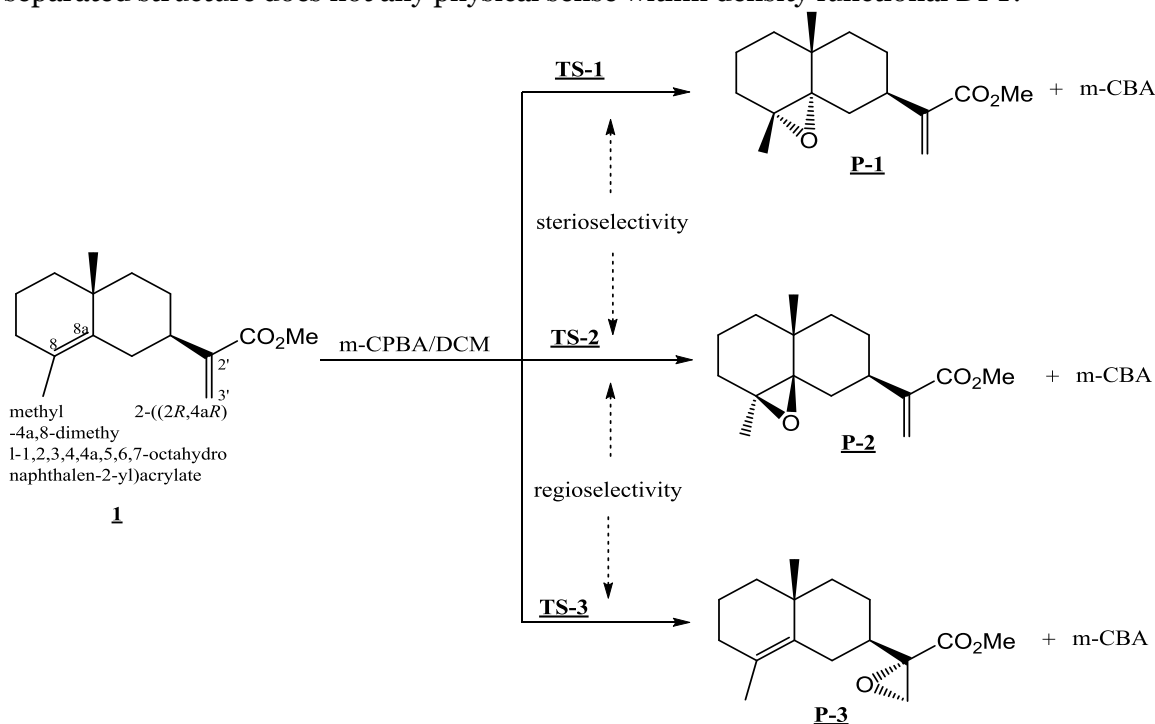


**Fig. 2.** Competitive regio- and stereoisomeric pathways associated with epoxidation reactions of the methyl 2-((2R,4aR)-4a,8-dimethyl-1,2,3,4,4a,5,6,7-octahydronaphthalen-2-yl)acrylate by m-CPBA

## 2. Computational methods

DFT computations were carried out using the B3LYP functional (Yanai et al 2004), together with the standard 6-31(d) basis set (Yanai et al 1982). The optimizations have been realized using the Bery analytical gradient optimization method. All computations have been shown with the Gaussian 09 suite of programs (Frisch et al 2009). The global electrophilicity index (Parr et al., 2009)  $\omega$ , was given by the following expression  $\omega = \frac{\mu^2}{2\eta}$ , in terms of the electronic chemical potential  $\mu$  and the chemical hardness  $\eta$ . Both quantities could be approached in terms of the one-electron energies of the frontier molecular orbital HOMO and LUMO,  $\epsilon_H$  and  $\epsilon_L$  as  $\mu = \frac{\epsilon_H + \epsilon_L}{2}$  and  $\eta = \epsilon_H - \epsilon_L$ , respectively. The empirical nucleophilicity index N (Domingo et al 2008; Domingo, Pérez 2011), based on the HOMO energies obtained within the Kohn-Sham (Kohn, Sham 1965), and defined as  $N = E_{HOMO}(Nu) - E_{HOMO}(TCE)$ . the nucleophilicity was referred to tetracyanoethylene (TCE). This choice allowed us to handle conveniently a nucleophilicity scale of positive values. Electrophilic  $P_k^+$  and nucleophilic  $P_k^-$  Par functions were obtained through analysis of the Mulliken atomic spin density (ASD) of the radical anion and radical cation of the reagents. The local electrophilicity and the local nucleophilicity indices were evaluated using the following expressions  $\omega_k = \omega P_k^+$  and  $N_k = N P_k^-$  (Ourhriss et al., 2018; El Haib et al., 2018; Ourhriss et al., 2017; El Idrissi et al., 2017; Zeroual et al., 2017; Zoubir et al., 2017; Zeroual et al., 2017; Zeroual et al., 2017; El Idrissi et al., 2017; Zoubir et al., 2016; Zeroual et al., 2016; El Idrissi et al., 2016; Zeroual et al., 2015; Barhoumi et al., 2015; Ryachi et al., 2015; Zeroual

et al., 2014; El Idrissi et al., 2013). The stationary points were characterized by frequency computations in order to verify that TSs have one and only one imaginary frequency. Intrinsic reaction coordinate (IRC) (Fukui, 1970) pathways were traced to verify the connectivity between minima and associated TSs.

### 3. Results and discussion

This theoretical study has been divided into three parts: (1) first, an analysis of the DFT reactivity indices of the reagents involved in these oxidation reaction; (2) then, a PES study of the reactions involved in this oxidation reactions are characterized and discussed; (3) finally, an analysis of the transition state structures are evaluated.

#### 3.1. DFT analysis based on the global and local reactivity indexes

In order to understand the mechanism of the oxidation reaction studied, we used DFT B3LYP/6-31G (d) to calculate the global indices shown in Table 1 the electronic chemical potential  $\mu$ , chemical hardness  $\eta$ , global electrophilicity  $\omega$  and nucleophilicity N of the methyl 2-((2R,4aR)-4a,8-dimethyl-1,2,3,4,4a,5,6,7-octahydronaphthalen-2-yl)acrylate **1** and m-CPBA

**Table 1.** Electronic chemical potential  $\mu$ , chemical hardness  $\eta$ , electrophilicity  $\omega$  and nucleophilicity N calculated using DFT B3LYP/6-31G (d) (eV)

System	$\mu$	$\eta$	$\omega$	N
<b>1</b>	-3.26	5.11	1.04	3.71
m-CPBA	-4.35	5.29	1.79	2.52

The electronic chemical potential of the ester **1**,  $\mu = -3.26$  eV, is higher than that of the m-CPBA,  $\mu = -4.35$  eV, thereby indicating that along a polar reaction the global electron density transfer (GEDT) will go from ester **1** towards the m-CPBA.

The ester **1** presents an electrophilicity  $\omega$  index of 1.04 eV and a nucleophilicity N index of 3.71 eV, being classified as strong nucleophile and  $\omega$  index of the m-CPBA, 1.79 eV and a nucleophilicity N index of 2.52 eV. Consequently, the m-CPBA is classified as a strong electrophile, while the ester **1** as a strong nucleophile.

Recently, the electrophilic and nucleophilic Parr functions have been proposed to analyse the local reactivity in polar processes involving reactions between a nucleophile/electrophile pair. Accordingly, the nucleophilic Parr functions, the density of the HOMO and LUMO orbitals for **1a** and **1** are represented in Figure 3.

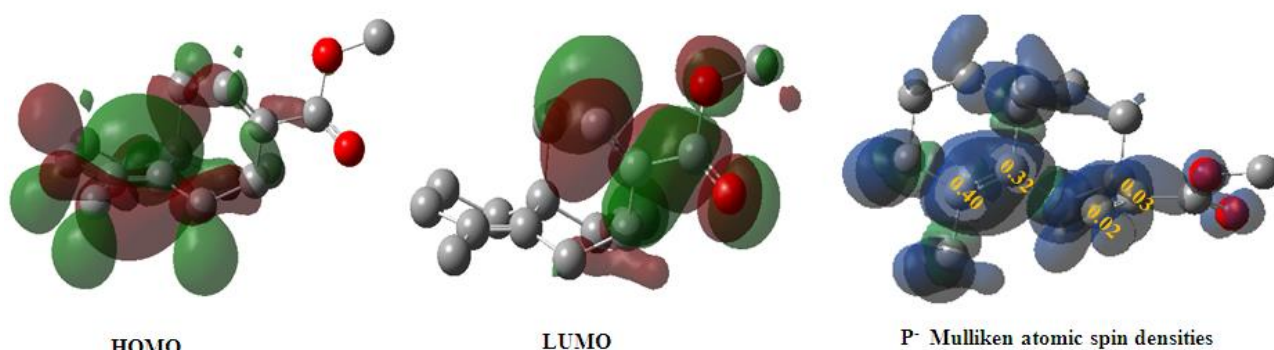


**Fig. 3.** Maps of the HOMO, LUMO orbital and nucleophilic Parr functions for **1**

From Figure 3, we find that:

The HOMO orbital of reagent **1** is highly condensed on the C8a = C8 double bond and the LUMO orbital is condensed on the C2 = C3' double bond, which shows that the nucleophilic power is condensed on the C8a = C8 double bond.

The Parr nucleophilic functions of the C8a (0.32) and C8 (0.40) carbons are greater than the Parr functions of the C2 (0.03) and C3' (0.02) carbons, which shows that the attack is very favorable at the level of double bond C8a=C8, this result is in good agreement with experience.

To confirm this result we conducted an energy study.

### 3.2 Energies study

Due to the non-symmetry of both ester **1**, epoxidation reaction of the ester (**1**) by m-CPBA can take place through three competitive reactive channels namely 1, 2 and 3 and to interpret the regio- and stereoselectivity experimentally observed in this epoxidation, the energies and relative energies were calculated and summarized in Table 2, PES of the reaction was calculated by B3LYP/6-31G(d) method. Intrinsic Reaction Coordinate (IRC) calculations were performed to characterize the transition states on the PES (Figure 4).

**Table 2.** B3LYP/6-31G (d) energies E (in a.u.) and relative energies ( $\Delta E$ , in kcal/mol) of the reagents, transition states and products.

System	E	$\Delta E$
1+m-CPBA	-1730,098803	-----
TS1	-1730,061794	23,22
P 1+m-CBA	-1730,187139	-55,43
TS 2	-1730,024362	46,71
P 2+m-CBA	-1730,196361	-61,21
TS3	-1730,045573	33,40
P 3+m-CBA	-1730,186418	-54,97

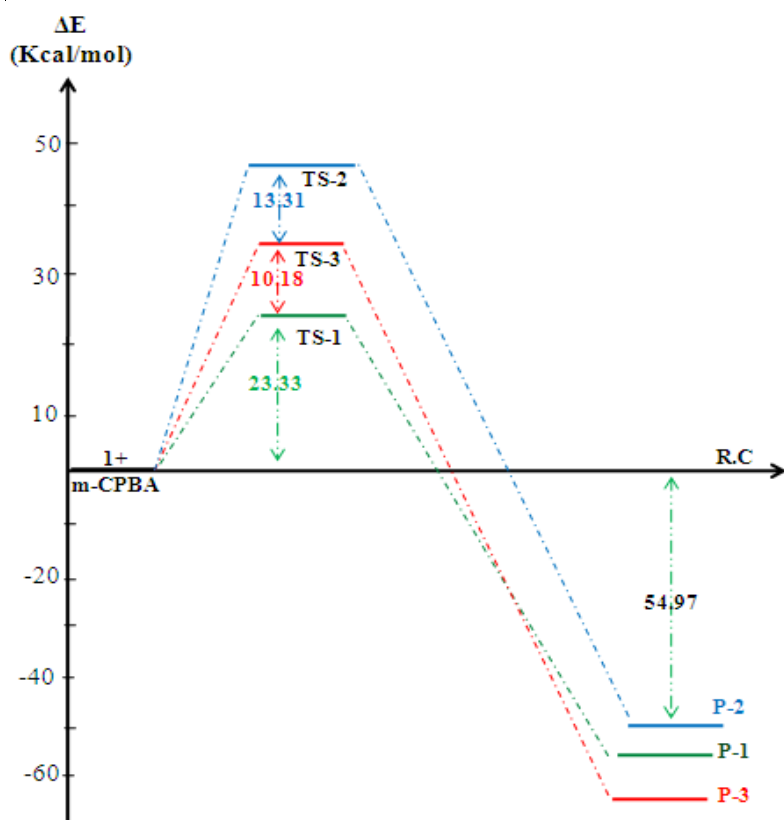


**Fig. 4.** Pathways for epoxidation reaction of the methyl 2-((2R,4aR)-4a,8-dimethyl-1,2,3,4,4a,5,6,7-octahydronaphthalen-2-yl)acrylate **1** and m-CPBA

We can see from Table 2 and Figure 4 that the activation energies of the products associated with the three reactive channels of the reaction between the methyl 2-((2R,4aR)-4a,8-dimethyl-1,2,3,4,4a,5,6,7-octahydronaphthalen-2-yl)acrylate **1** and m-CPBA are 23.22, 46.71 and 33.40 for TS1, TS2 and TS3 respectively, indicating that the formation of product P1 **1**, was kinetically preferred, the difference between TS1 and TS3 is 10.18 (eV) and TS1 and TS2 is 23.49 (eV) which shows that the formation of the complexes P2 and P3 is impossible.

Other hand the formation of the compounds P1, P2 and P3 are exothermic by 55.43, 61.21 and 54.97 indicating that the complex P2 is more stable than P1 and P3, which shows that the formation of the product P1 is kinetically favorable in good agreement with the experimental results.

### 3.3. Geometries study

The geometries of the TSs involved in the three competitive reaction channels are given in Fig. 3. At the TSs, the lengths of the C8–O and C8a–O forming bonds are 1.482 and 1.495 Å (TS-1) and , the lengths of the C8–O and C8a–O forming bonds are 2.589 and 2.714 Å (TS-2), and the lengths of the C3'–O and C2'–O forming bonds are 2.006 and 2.418 Å (TS-3). Some appealing conclusions can be drawn from these geometrical parameters: (1) the TSs associated with the 1 channels are more asynchronous than those associated with the other one.

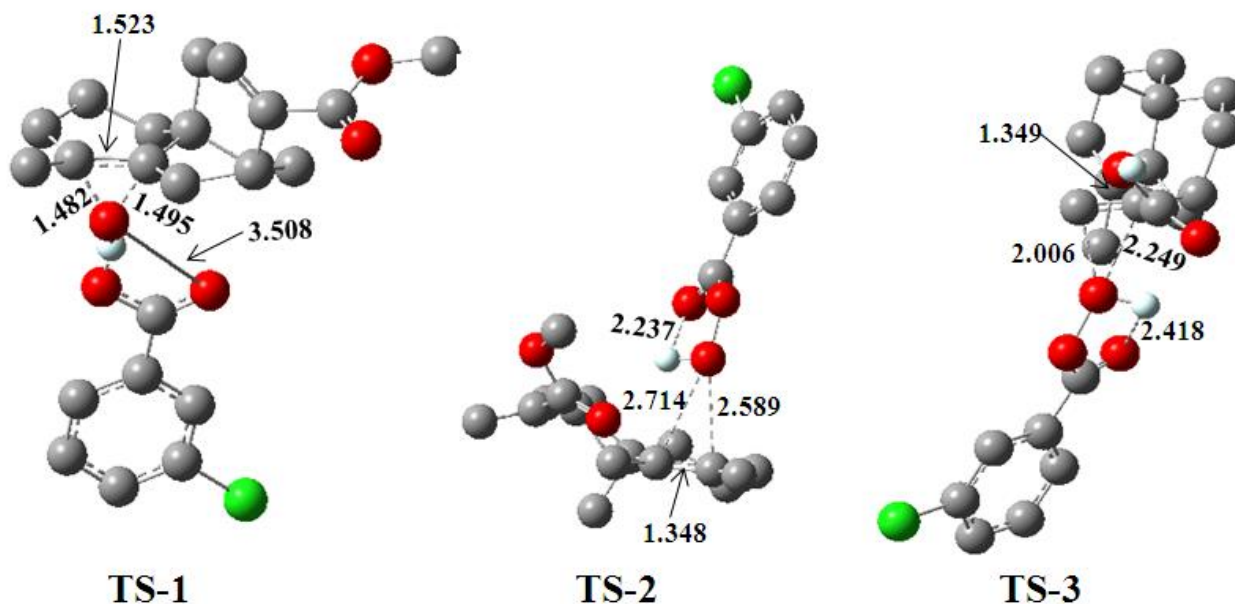


**Fig. 3.** DFT/6-31G(d) optimized density map and structures of the TSs of the epoxidation reaction of the methyl 2-((2R,4aR)-4a,8-dimethyl-1,2,3,4,4a,5,6,7-octahydronaphthalen-2-yl)acrylate **1** and m-CPBA. Lengths are given in Angstroms.

### 4. Conclusion

The regioselectivity and the nature of the molecular mechanism of the epoxidation reaction of the methyl 2-((2R,4aR)-4a,8-dimethyl-1,2,3,4,4a,5,6,7-octahydronaphthalen-2-yl)acrylate **1** by m-CPBA have been theoretically studied using DFT methods at the B3LYP/6-31G(d) level of theory. Three reactive channels corresponded to the 1, 2 and 3 regio and stereoselective approach modes have been explored and characterized for the methyl 2-((2R,4aR)-4a,8-dimethyl-1,2,3,4,4a,5,6,7-octahydronaphthalen-2-yl)acrylate **1**. We can summarize the results of the present study in the following points:

Analysis of the computed nucleophilic Parr functions of the nucleophilic 2-((2R,4aR)-4a,8-dimethyl-1,2,3,4,4a,5,6,7-octahydronaphthalen-2-yl)acrylate **1** indicates that the double bond C<sub>8</sub>=C<sub>8a</sub> is the most nucleophilic centers, justifying the regioselectivity obtained experimentally

The formation of the compounds P1, P2 and P3 are exothermic by 55.43, 61.21 and 54.97 indicating that the complex P2 is more stable than P1 and P3, which shows that the formation of the product P1 is kinetically favorable in good agreement with the experimental results.

### References

- Barbetti et al., 1985 – Barbetti P., Chiappini I., Fardella G., Menghini A. (1985). A New Eudesmane Acid from *Dittrichia* (*Inula*) viscosa. *Planta Med.*, 51(5): 471.
- Barhoumi et al., 2015 – Barhoumi A., Zeroual A., Bakkas S., El Hajbi A. (2015). Theoretical study of the regioselectivity of the reaction between tetrachloromethane and triethyl phosphite

using the DFT B3LYP/6-31G (d) method". *Journal of Computational Methods in Molecular Design*, 5 (2), 8-15.

[Domingo et al 2008](#) – Domingo, L.R., Chamorro, E., Pérez, P. (2008). Understanding the Reactivity of Captodative Ethylenes in Polar Cycloaddition Reactions. A Theoretical Study, *J. Org. Chem*, 73: 4615-4624.

[Domingo 2014](#) – Domingo, L.R. (2014). A new C–C bond formation model based on the quantum chemical topology of electron density. *RSC Adv.*, 4: 32415–32428.

[Domingo et al., 2016](#) – Domingo, L.R., Ríos-Gutiérrez, M., Pérez, P. (2016). A new model for C–C bond formation processes derived from the Molecular Electron Density Theory in the study of the mechanism of [3+2] cycloaddition reactions of carbenoid nitrile ylides with electron-deficient ethylenes. *Tetrahedron*, 72: 1524–1532.

[Fraga., 2007](#) – Fraga B.M. (2007). Natural sesquiterpenoids, *Nat. Prod. Rep.*, 24, 1350–1381.

[El Haïb et al., 2018](#) – El Haïb A., Elajlaoui R., El Idrissi M., Moumou M., Abouricha S., Zeroual A., Benharref A., El Hajbi A. (2018). The mechanism, the chemoselectivity and the regioselectivity of the 1-Benzyl-4-ethynyl-1H-[1,2,3]triazole and 1-Azidomethyl-4-tert-butylbenzene in [3+2] cycloaddition reactions: a DFT study. *Mor. J. Chem.* 6(1), 14-21.

[El Idrissi et al., 2016](#) – El Idrissi M., Zoubir M., Zeroual A., El Ajlaoui R., El Haïb A., Benharref A., El Hajbi A. (2016). A theoretical study of the mechanism and regioselectivity of the 1,3-dipolar cycloaddition reaction of azides with alkynes. *Journal Marocain de Chimie Hétérocyclique*, 15 (1), 146-151.

[El Idrissi et al., 2016](#) – El Idrissi M., El Haïb A., Zoubir M., Hammal R., Zeroual A., El Hajbi A. (2016). Understanding the regioselectivity of the Baeyer-Villiger reaction of bicyclo[4.2.0]octan-7-one and bicyclo[3.2.0]heptan-6-one: A DFT Study. *Journal of Computational Methods in Molecular Design.*, 6 (3), 75-79.

[El Idrissi et al., 2017](#) – El Idrissi M., El Ajlaoui R., Zoubir M., Abouricha S., Moumou M., Zeroual A., Benharref A., El Hajbi A. (2017). Theoretical study of the chemo- and regioselectivity of the [3+2] cycloaddition reaction between mesitronitrile oxides and 2-fluoren-9-ylidene-malononitrile. *J. Mater. Environ. Sci.*, 8 (10), 3564-3569.

[El Idrissi et al., 2017](#) – El Idrissi M., Zeroual A., El Haïb A., Benharref A., El Hajbi A. (2017). Theoretical study of the mechanism and regioselectivity of electrophilic substitution reaction between the ar-himachalene and acetic anhydride. *International Journal of Multidisciplinary Sciences*, (2), 1-10.

[El Idrissi et al., 2013](#) – El Idrissi M., Zeroual A., Benharref A., El Hajbi A. (2013). Determination of certain thermodynamic and geometric values and condensation mechanism of  $\beta$ -himachalene and dibromocarbene using density functional theory (DFT). *Phys. Chem. News*, 69, 89-95.

[El Idrissi et al., 2017](#) – El Idrissi M., Zoubir M., Zeroual A. (2017). Understanding the mechanism and regioselectivity of Prop-2-yn-1-ol with azido-compounds in [3+2] cycloaddition reactions: a molecular electron density theory study. *Journal Marocain de Chimie Hétérocyclique*, 16 (1), 179-185.

[Francl et al 1982](#) – Francl, M.M., Pietro, W.J., Hehre W.J. (1982). A polarization-type basis set for second-row elements. *J. Chem. Phys.*, 77: 3654-3665.

[Frisch et al., 2009](#) – Gaussian 09, Revision A.02, Frisch M. J. et al.

[Fukui, 1970](#) – Fukui, K. (1970). Formulation of the reaction coordinate. *J. Phys. Chem*, 74: 4161–4163.

[Ourhriss et al., 2018](#) – Ourhriss N., Zeroual A., Gadhi C. A., Benharref A., Abourriche A., Bennamara A., El Hajbi A. (2018). A Regioselective and Stereoselective Synthesis of 2,5-Dichloro-2,5,9,9-tetramethyl-decahydro-benzocycloheptene via Stepwise addition Reactions between  $\alpha$ -himachalene and HCl: Experimental and Theoretical Study. *European Reviews of Chemical Research*, 5(1), 22-29.

[Ourhriss et al., 2017](#) – Ourhriss N., Zeroual A., Gadhi C. A., Benharref A., Abourriche A., Bennamara A., El Hajbi A. (2017). Synthesis, spectroscopic NMR and theoretical (HF and DFT) investigation of 3,5,5,9-tetramethyl-2-nitro-6,7,8,9-tetrahydro-5H-benzocycloheptene and 2,5,9,9-tetramethyl-1,3-dinitro-6,7,8,9-tetrahydro-5H-benzocycloheptene. *European Journal of Molecular Biotechnology*, 5(2), 52-59.

[Ourhriss et al., 2017](#) – Ourhriss N., Zeroual A., Ait ElHad M., Mazoir N., Abourriche A., Gadhi C.A., Benharref A., El Hajbi A. (2017). Synthesis of 1-isopropyl-4,7-dimethyl-3-nitronaphthalene: An experimental and theoretical study of regiospecific nitration. *J. Mater. Environ. Sci.*, 8 (4), 1385-1390.

[Ryachi et al., 2015](#) – Ryachi K., Zeroual A., Khamliche L., Bakkas S., El Hajbi A. (2015). Understanding the regioselectivity and reactivity of some ethylene compounds using Parr functions. *J. Nat. Prod. Plant Resour.*, 5 (3), 18-22.

[Shtacher, Kashman, 1970](#) – Shtacher G., Kashman Y. (1970). 12-Carboxyeudesma-3,11(13)-diene. Novel sesquiterpenic acid with a narrow antifungal spectrum) and anti-inflammatory activity. *J. Med. Chem.*, 13 (6), 1221-1223.

[Yanai et al 2004](#) – Yanai, T., Tew, D.P., Handy, N.C. (2004). A new hybrid exchange? correlation functional using the Coulomb-attenuating method (CAM-B3LYP). *Chemical Physics Letters*, 393: 51-57.

[Zaki et al., 2017](#) – Zaki M., Akssira M., Berteina-Raboin S. (2017). Modification of Natural Eudesmane Scaffolds via Mizoroki-Heck Reactions, *Molecules*, 22, 652.

[Zeroual et al., 2017](#) – Zeroual A., El Idrissi M., Zoubir M., El Ajlaoui R., Abouricha S., El Hajbi A. (2017). Theoretical Study of the Mechanism and Regioselectivity of Prop-2-Yn-1-Ol with Azide in [3+2] Cycloaddition Reactions. *Open Access Journal of Translational Medicine & Research*, 1(1), 1-5.

[Zeroual et al., 2017](#) – Zeroual A., El Idrissi M., Zoubir M., Benharref A. (2017). Theoretical study of the reactivity and regioselectivity of the addition reaction between HCl and alkenes, investigation of the Markovnikov's rule. *European Reviews of Chemical Research*, 4(1), 21-27.

[Zeroual et al., 2017](#) – Zeroual A., El Idrissi M., El Ajlaoui R., Ourhriss N., Abouricha S., Mazoir N., Benharref A., El Hajbi A. (2017). MEDT study of the mechanism and regioselectivity of diazocompounds and alkenes in [3+2] cycloaddition reaction". *European Journal of Molecular Biotechnology*, 5(1), 43-49.

[Zeroual et al., 2017](#) – Zeroual A., Zoubir M., El Idrissi M., El Ajlaoui R., El Haib A., Abouricha S., Mazoir N., El Hajbi A. (2017). Theoretical Analysis of Reactivity and regioselectivity in [1+2] cycloaddition reaction of limonene, terpinolene and  $\gamma$ -terpinene with dichlorocarbene. *Global Journal of Science Frontier Research: B, Chemistry*, 17(1).

[Zeroual et al., 2016](#) – Zeroual A., Hammal R., Benharref A., Mazoir N., El Hajbi A. (2016). A theoretical investigation of the reactivity and regioselectivity of triterpene derivatives using difference local index, Parr functions and a difference of Parr functions, *Mor. J. Chem.* 4 (4), 938-944.

[Zeroual et al., 2015](#) – Zeroual A., Mazoir N., Benharref A., El Hajbi A. (2015) "Understanding of the stereoselective epoxidation on triterpene derivative using transition state theory". *Journal of Computational Methods in Molecular Design.*, 5 (4), 158-161.

[Zeroual et al., 2015](#) – Zeroual A., Hammal R., El Hajbi A. (2015). A DFT Study of the [1+2] Cycloaddition Reactions of 2-[1, 3]Dioxolan-2-ylidene-malononitrile, TCE and chlorocarbene. *Journal of Computational Methods in Molecular Design.*, 5 (4), 97-101.

[Zeroual et al., 2015](#) – Zeroual A., El Hajbi A. (2015). Understanding the regioselective and molecular mechanism of the TCE in cycloaddition reaction (TCE+Cp) and addition reaction (TCE+HCl) using DFT calculation". *Canadian Chemical Transactions*, 3 (4), 430-437.

[Zeroual et al., 2015](#) – Zeroual A., Hammal R., Benharref A., El Hajbi A. (2015). The regio- and stereoselective addition of dibromocarbene and dichlorocarbene onto  $\beta$ -himachalene" *Mor. J. Chem.*, 3(4), 698-704.

[Zeroual et al., 2015](#) – Zeroual A., Barhoumi A., Bakkas S., El Hajbi A. (2015). Understanding, which oxygen attacks bromotrimethylsilane in McKenna Reaction using DFT calculation? *Journal of Computational Methods in Molecular Design*, 5 (3), 150-154.

[Zeroual et al., 2015](#) – Zeroual A., El Haib A., Benharref A., El Hajbi A. (2015). A Combined Experimental and Theoretical Study of highly chemoselectivity acetylation of diterpene. *Journal of Computational Methods in Molecular Design*, 5 (3), 58-62.

[Zeroual et al., 2015](#) – Zeroual A., Zoubir M., Hammal R., Benharref A., El Hajbi A. (2015). Understanding the regioselectivity and reactivity of Friedel–Crafts benzoylation using Parr functions". *Mor. J. Chem.*, 3(2), 356-360.

[Zeroual et al., 2015](#) – Zeroual A., Benharref A., El Hajbi A. (2015). Theoretical study of stereoselectivity of the [1+2] cycloaddition reaction between (1S,3R,8S)-2,2-dichloro-3,7,7,10-

tetramethyltricyclo[6,4,0,01.3]dodec-9-ene and dibromocarbene using density functional theory (DFT) B3LYP/6-31G\*(d). *Journal of Molecular Modeling*, 21 (3), 1610-2940.

Zeroual et al., 2014 – Zeroual A., Hammal R., Benharref A., El Hajbi A. (2014). A theoretical investigation of the regio- and stereoselectivities of the  $\beta$ -himachalene. *Journal of Computational Methods in Molecular Design*, 4 (3), 106-112.

Zeroual et al., 2014 – Zeroual A., Hammal R., Ryachi K., Barhoumi A., Benharref A., El Hajbi A. (2014). Understanding the Regioselectivity and Reactivity of  $\beta$ -Himachalene Using Zeroual Function as a new Regioselectivity Descriptor. *International Journal of Innovation and Applied Studies*, 8 (2), 750-755.

Zeroual et al., 2014 – Zeroual A., El Idrissi M., Benharref A., El Hajbi A. (2014) Theoretical study of regioselectivity and stereoselectivity of condensation of  $\beta$ -himachalene with dichlorocarbene using density functional theory (DFT). *International Journal of Innovation and Applied Studies*, 5 (2), 120- 130.

Zoubir et al., 2017 – Zoubir M., El Idrissi M., El Ajlaoui R., El Haib A., Zeroual A., Benharref A., El Hajbi A. (2017). Theoretical study of the chemo and the regioselectivity of the Baeyer-Villiger reaction of bicyclo[3.2.0]hept-2-en-6-one by hydrogen peroxide. *European Reviews of Chemical Research*, 4(1), 28-33.

Zoubir et al., 2017 – Zoubir M., Zeroual A., El Idrissi M., Bkiri F., Benharref A., Mazoir N., El Hajbi A. (2017). Experimental and theoretical analysis of the reactivity and regioselectivity in esterification reactions of diterpenes (totaradiol, totaratriol, hinikione and totarolone). *Mediterranean Journal of Chemistry*, 6(4), 98-107.

Zoubir et al., 2017 – Zoubir M., Zeroual A., El Idrissi M., El Haib A., Moumou M., Hammal R., Mazoir N., Benharref A., El Hajbi A. (2017). Understanding the chemoselectivity and stereoselectivity in Michael addition reactions of  $\beta$ -hydroxypartenolides and amines such as pyrrolidine, morpholine, piperidine and 1-methylpiperazine: a DFT study. *J. Mater. Environ. Sci.*, 8(3), 990-996.

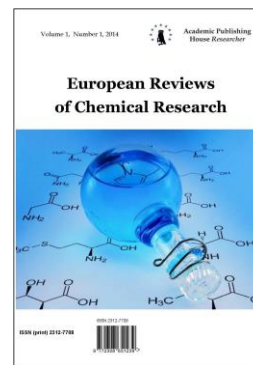
Zoubir et al., 2016 – Zoubir M., Zeroual A., Benharref A., El Hajbi A. (2016). Understanding the Holleman Rule in the Electrophilic Substitution Reaction Using Parr Functions. *Journal of Computational Methods in Molecular Design*, 6 (4), 1-4.

Copyright © 2018 by Academic Publishing House Researcher s.r.o.



Published in the Slovak Republic  
European Reviews of Chemical Research  
Has been issued since 2014.  
E-ISSN: 2413-7243  
2018, 5(2): 67-74

DOI: 10.13187/erchr.2018.2.67  
[www.ejournal14.com](http://www.ejournal14.com)



## Impact Studies of Pest Control Products used in Closed Production Environments on Food Production Quality by SPME coupled to GC-MS

A. Lakhili<sup>a,b</sup>, M. Fekhaoui<sup>b</sup>, A. Bellaouchou<sup>b</sup>, L. Tahri<sup>b</sup>, A.E. Abidi<sup>b</sup>, M. El idrissi<sup>c,\*</sup>

<sup>a</sup>National Institute of Hygiene, Rabat, Morocco

<sup>b</sup>Mohammed V University, Rabat, Morocco

<sup>c</sup>Chouaïb Doukkali University, El Jadida, Morocco

### Abstract

To determine concentration insecticides and rat poisons detected in the finished industrial samples, the solid phase micro extraction (SPME) is applied. The gas chromatography coupled to a mass spectrum (GC-MS) is elaborated. In order to get a best extraction, different process parameters are examined and optimized. The relevant finding are obtained using a time of unspecific binding properties of 30 minutes duration and mode of agitation for 30 min with agitation by magnetic stirrer and a temperature of 30° C. It has been demonstrated that insecticides, rat poisons and pesticides have a high chance of being found at a high concentration in finished industrial products.

**Keywords:** GC-MS; SPME; extraction; Performance; rat poisons; insecticides.

### 1. Introduction

Pesticides (rat poisons and insecticides) are compounds characterized by their diversity and their different physicochemical properties (Blasco et al., 2004). Their adverse side effects have been quickly identified. It turns out that the toxicity related to their molecule structures is, in principle, not limited due to the associated species which should be evinced. It has been shown that they are particularly toxic not only to humans (Bonansea et al., 2013; Jones et al., 2012) but also to the environment. These molecules tend to accumulate in different biotic and abiotic matrices, including water, air, soil, aquatic organism, blood and food (Dong et al., 2003; Hlotz et al., 2004). It is noted that pesticides are among the oldest organic synthetic ones being used in the agriculture activities in the world since 1940 because of their strong impact in the fight against pests and diseases (Jelen et al., 2012; Hays et al., 2003). However, pesticides are very toxic and persistent in the environment which tends to accumulate in living organisms. Following to low degradation and high solubility in organic materials, they easily enter the food chain as contaminants reaching humans through the consumption of drinking water and agricultural food products (Tanabe et al., 1993; Kirrluk et al., 1995). Although most of them have been banned from use, however, they are still detected in ecosystems (Kosikowska et al., 2010; Svjetlana et al., 2010; Raposo et al., 2007; Rianawati et al., 2009; Mesquita et al., 2011).

Recently, the analysis of pesticide residues has received increasing attention in many places including in north African countries. In particular, it has been remarked that the pesticides

\* Corresponding author

E-mail addresses: [idrissi\\_82@hotmail.fr](mailto:idrissi_82@hotmail.fr) (M. El idrissi)

monitoring in industrial products is very important and requires high efficiency, unique selectivity, and high sensitivity techniques (Vidal et al., 2009; Shahsavand et al., 2018).

In agribusiness industries, the use of pesticides (rat poisons and insecticides) in the treatment of production and storage areas eliminates the pests that may be developed and impaired the quality of the finished products or the production process. The latter is framed by the law and controlled by the ONSSA (National Office of Sanitary Safety of Food Products) within the framework of an effective normative use of such chemical products without an impact on industrial food products ready for consumption.

In this present work, we first verify the impact of the use of these products (rat poisons, insecticides) used to treat pests in closed industrial areas (storage areas, production areas). Then, we check the presence or the absence of traces and concentrations of these products in the finished products. For this purpose, we adopt the method of the micro-extraction on the solid phase SPME, in the presence of the chromatography gas coupled to a mass spectrum (GC-MS). This coupling SPME/GC-MS provides a great sensitivity and precision even at very low concentration.

## 2. Materials and methods

In this section, we give the essential on the used methods including materials.

### 2.1 SPME solid phase micro-extraction method

For the detection and the quantification of molecules of the industrial products by the solid phase microextraction method (SPME), we immersed the SPME fiber in the studied samples. This step was carried out at room temperature for 15 minutes. It can be illustrated in (Figure 1).

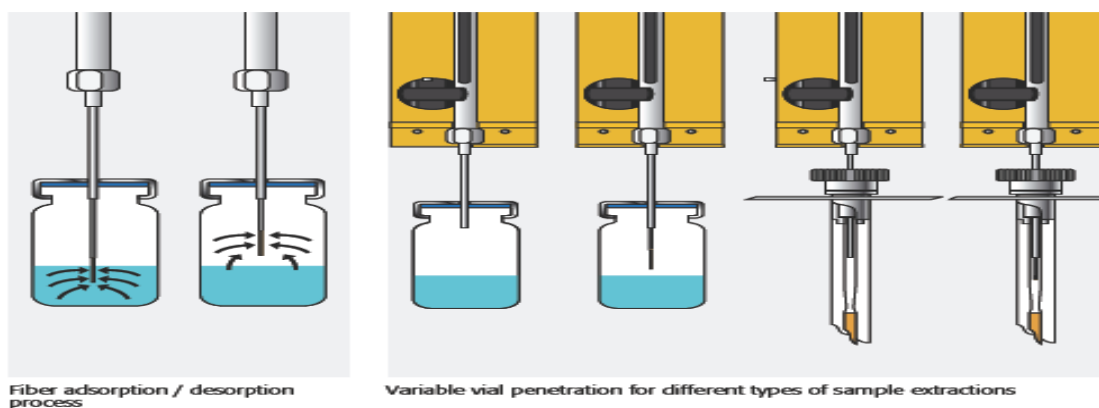


**Fig. 1.** Adsorption and desorption process by SPME

The used fiber consists of a Carboxen/PDMS/DVB 50/30  $\mu\text{m}$  phase. The chemical compounds are first concentrated on the fiber (adsorption phase), then they are thermally desorbed in the GC-ECD injector. The analysis conditions are the same as the ones mentioned above (Anandhakumar et al., 2013).

### 2.2 Optimizing SPME

To increase the sensitivity and the effectiveness of the SPME method, we considered an optimization of various parameters such as the temperature, the exposure time, the duration and the mode of agitation, the effect of the pH and adding salt.

### 2.3 Calculation method

The concentration is determined according to the method of qualification of the peaks taking into account the volume of final extract and the volume of sample analyzed for each identified molecule. For the SPME method, it is given by

$$C_e = \frac{A_e \times C_i}{A_{st}}$$

Where  $C_e$  is the concentration of a compound in the sample.  $A_e$  indicates the area of a compound in the sample.  $A_{st}$  is the area of a compound in the standard.  $C_i$  represents initial concentration of a compound in the standard and  $V$  denotes the volume of the sample to be dosed

in ml.  $V_e$  is the volume of extract in ml. The percent recovery (PR%) or yield of each compound was calculated using peak air. Concretely, this has been done using the following equation

$$PR = \frac{C_e}{C_i} \times 100$$

Where  $C_e$  now represents the concentration of the sample and where  $C_i$  denotes the standard initial concentration.

### 3. Results and discussions

In this section, we present the obtained results and the corresponding discussions. Before giving the main results of this work, we first check the stability and the validity of the studied method. It is recalled that the validation of an analytical method consists of the determination relevant parameters as the fidelity which itself represents a set of dispersion characteristics including repeatability, intermediate fidelity and reproducibility.

As a criterion for estimating the stability, we decide to elaborate a repeatability examination. It refers to test the same performed size under conditions as stable as possible and at short intervals. This measurement of the variation of the results should do in the same laboratory characterizes. The precision is obtained when the method is repeated by the same investigator under the same conditions (reagents, equipment, adjustment and laboratory) in a short time interval. This makes it possible to evaluate the accuracy of the method under the normal operating conditions.

To study the stability of SPME, a series of five repetitions analysis was performed on the chemical compost concentration ( $5\mu\text{g/L}$ ) under optimized conditions. The obtained results are shown (Figure 2).

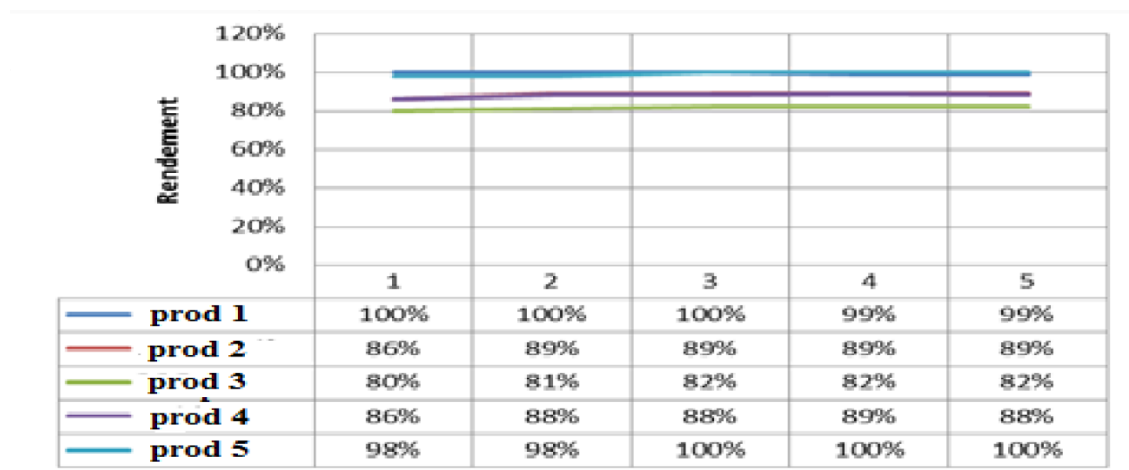


**Fig. 2.** Variation stability of SPME a series of five repetitions analysis was performed on the chemical compost concentration ( $5\mu\text{g/L}$ )

From Figure 2, it can be seen that for each products there is no variation with the identical yield values for all tests.

Having discussed the stability of five products, we present now the results and give the corresponding discussions. The industrial studied areas are given (Figure 3).

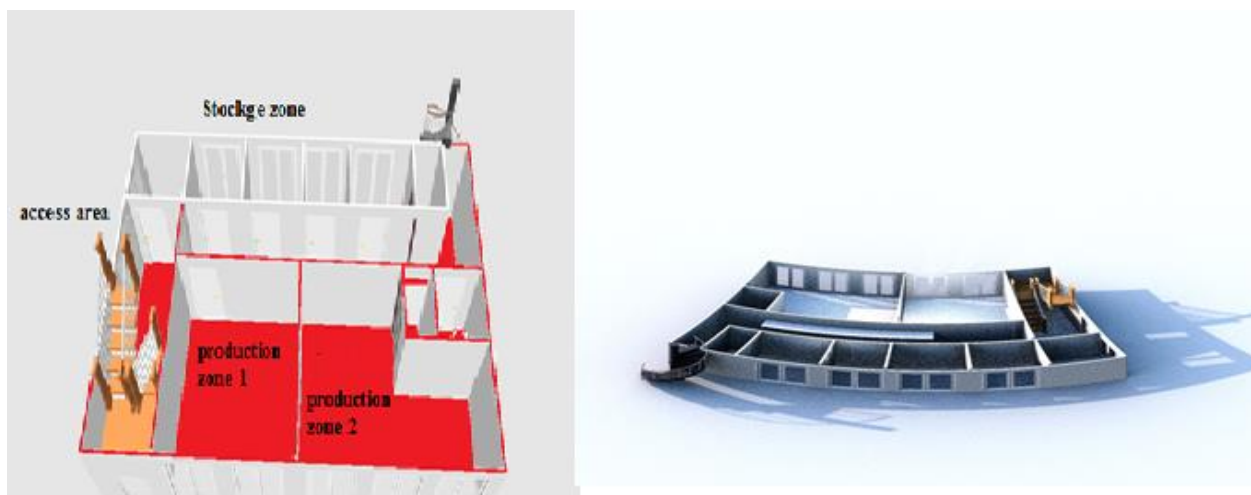


**Fig. 3.** Overall scheme of the building of products and storage treated by chemicals

Production areas (ZONE 1 and ZONE 2) were treated by spraying a liquid insecticide at the end of production at 9 pm. The treated products are illustrated in (Figure 4).

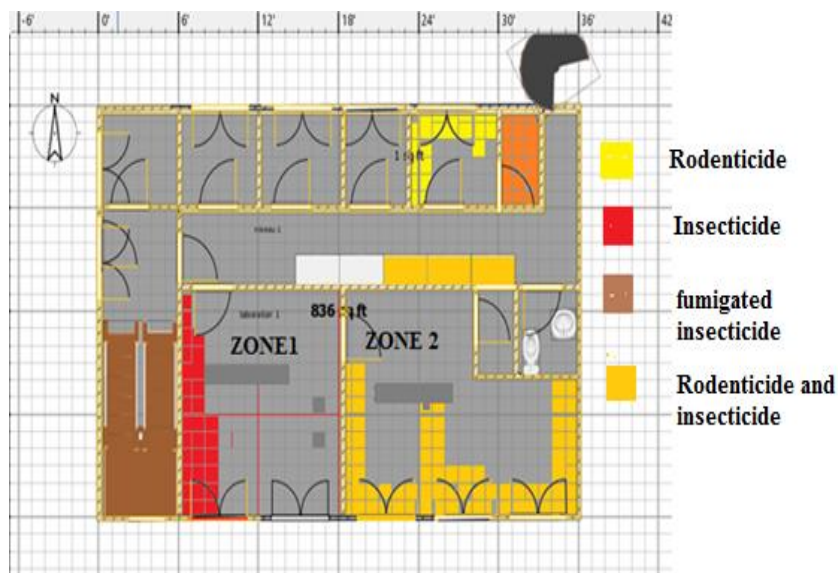


**Fig. 4.** Distribution of treatment areas by type of product used

Several varieties of insecticide insecticides were used in this study. In particular, we started by profiling the active ingredient of each industrial formulation (rat poison/insecticide). To be able to subsequently identify them, an analysis study should predormed. Indeed, samples are taken randomly in all the products before and after the surface treatment to see the impact of the treatment in the quality of the finished products.

After treatment, the SPME fiber was implanted at the outlet of the oven on the cooking belt to take advantage of the optimal adsorption condition already established in our preliminary study of implementation of the technique.

The following results represent the analytical profiles of the different peaks found by SPME/GC analysis: MS

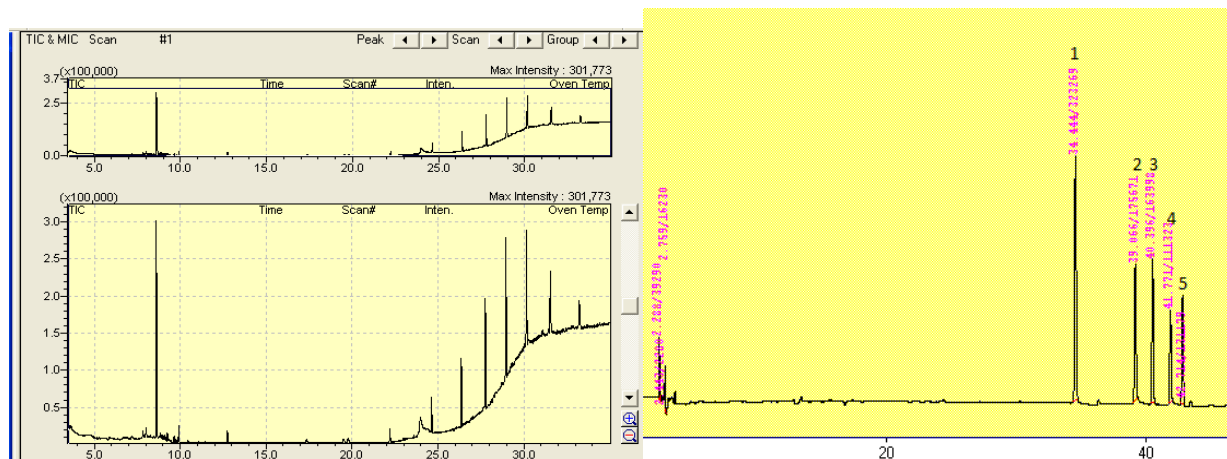


**Fig. 5.** Profile of the treatment product obtained by SPME coupled with GC-MS and GC-ECD

This figure represents the profile of the different chemical molecules that are present in the industrial formulation for insect treatment analyzed by SPME coupled to a GC-ECD and GC-MS.

In what follows we discuss the product analysis after 6 hours spent from the moment of surface treatment with insecticide raticides. The [Figure 6](#) represents the results obtained after analysis of the food products produced in zone 1 after 6 hours of the surface treatment.

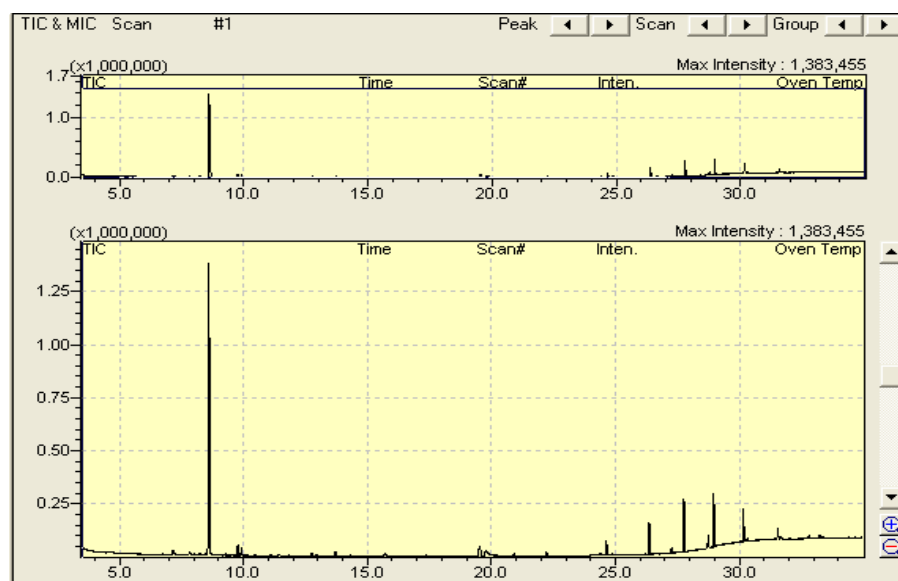


**Fig. 6.** Analysis results of the finished product by SPME coupled to GC-MS after 6 hours of treatment

After 6 hours of the surface treatment by pesticides and rat poisons by spraying, it has been noticed the presence of a low concentration of certain chemical products. This implies that the 6 hour delay is not sufficient to eliminate such chemical production after a spray.

The results obtained by SPME coupled to GC-MS after analysis of industrial production in a firm surface after 12 hours of surface treatment by spraying are illustrated in ([Figure 7](#)).

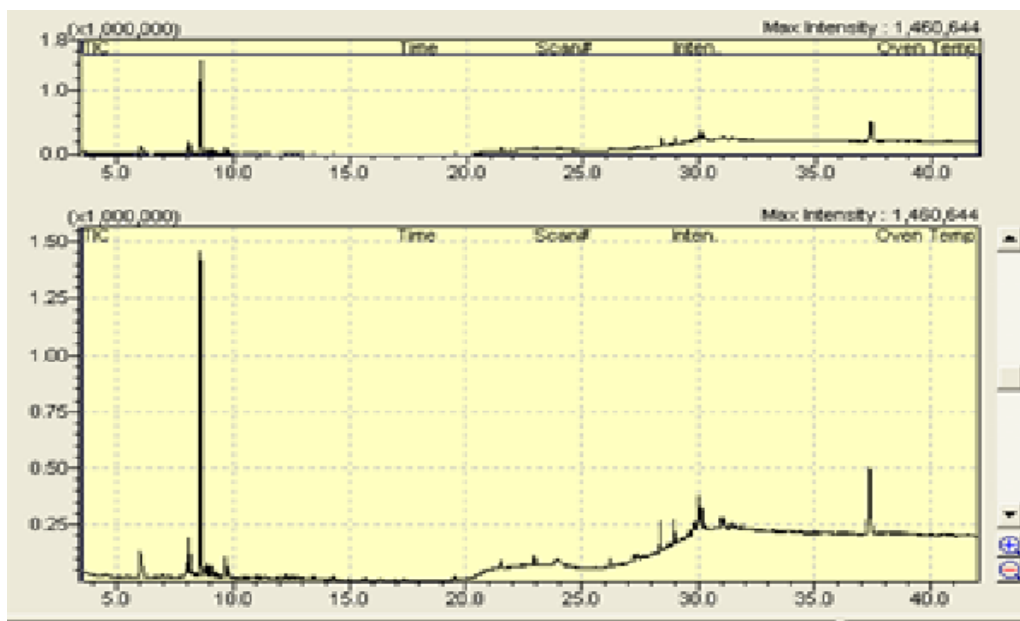


**Fig. 7.** Analysis results of the finished product by SPME coupled to GC-MS after 12 hours of treatment

After 12 hours of surface treatment, we found two molecules having very low concentration. It has been shown that the resumption of production after 12 hours of surface treatment can present risks on the quality of the finished product. The results obtained by SPME coupled to GC-MS after analysis of industrial production in a firm surface after 18 hours of surface treatment by spraying are given in (Figure 8).

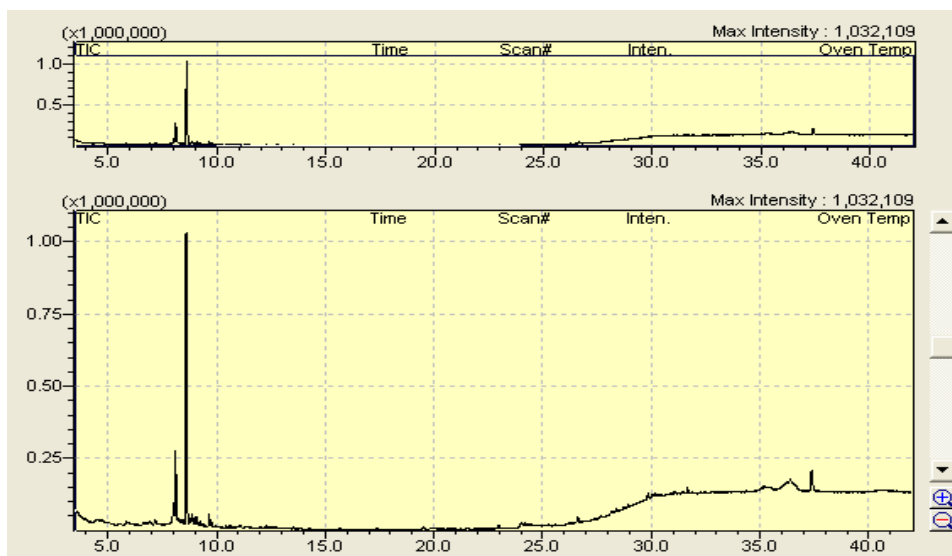


**Fig. 8.** Analysis results of the finished product by SPME coupled to GC-MS after 18 hours of treatment

It is noted that after 18 hours of surface treatment the presence of surface treatment products in the finished industrial products is very low or ignored. This allows us to think that 18h remains a minimum period of time of product to avoid the presence of the no desirable chemical element in the industrial production.

The results obtained by SPME coupled to GC-MS after analysis of industrial production in a firm surface after 24 hours of surface treatment by spraying are illustrated in (Figure 9).

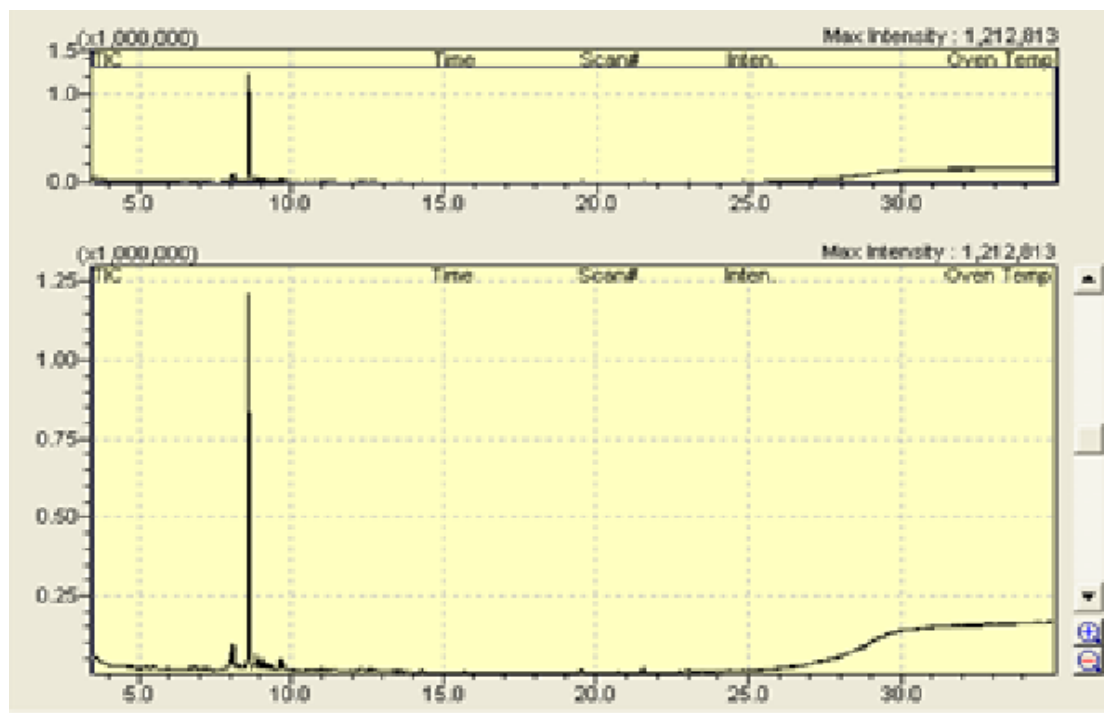


**Fig. 9.** Analysis results of the finished product by SPME coupled to GC-MS after 24 hours of treatment

After 24 hours of surface treatment, it is noted the total absence in the analysis.

We have worked on several pest control products that are used for the treatment of closed production surfaces and the impact of the use of these products on the quality of production on everything in the field agribusiness. Several industrial formulation profiles of insecticides and rat poisons were developed using the SPME technique coupled to GC-MS with repeatability and reproducibility to establish and verify the validity of the analytical method adopted. The present study respects the ISO quality norms. It has been observed that the use of these products may have a negative impact on the quality of the agri-food production of the units treated by chemical spraying on everything in the first 6 hours after treatment.

It has also been remarked that the use of SPME coupled to GC-MS in routine quality analyzes is very interesting, economical, efficient, stable in repeatability and reproducibility. It allows for accurate identification of all elements present at different concentrations even at the sample trace states.

#### 4. Conclusion

In this work, we have studied that the impact of the use of these products (rat poisons, insecticides) used to treat pests in closed industrial areas (storage areas, production areas). In particular, we checked the presence or the absence of traces and concentrations of these products in the finished products by using the method of the micro-extraction on the solid phase SPME, in the presence of the chromatography gas coupled to a mass spectrum (GC-MS).

After different analysis are carried out by SPME coupled to the GC-MS on sample product in a closed environment treated by products of rat extermination/disinsection taken at different times per palliate of 6 hours according to the iso quality standard adopted by the agri-food production. It has been shown that the interval of 18 h of stopped production after each chemical treatment is necessary to avoid the presence of any treatment product in the production. Moreover, it consequently avoid the alteration of the finished product. In this work, it has been observed that the coupling SPME/GC-MS provides a great sensitivity and precision even at very low concentration.

## 5. Conflict of Interest

The authors declare that there is no conflict of interests regarding the publication of this paper. Also, they declare that this paper or part of it has not been published elsewhere.

## References

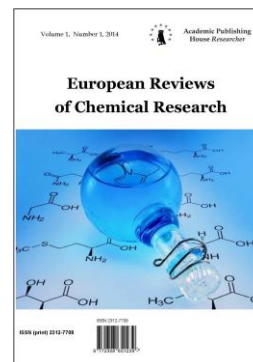
- Blasco et al., 2004 – Blasco C., Fernández M., Font Y.P.G., Chromato J.A. 1030, 77-85.
- Bonansea et al., 2013 – Bonansea R.I., Amé M.V., Wunderlin D.A. *Chemosphere*, 90, 1860-1869.
- Jones et al., 2012 – Jones K.C.D. *Environ. Sci. Technol.*, 46, 1396-1405.
- Dong et al., 2003 – Dong R.A., Liao P.L., Chromato J. A, 918, 177-188.
- Hlotz et al., 2004 – Dougherty C.P., Hlotz S.H., Reinert J.C., Panyacosit L., Axelrad D.A., Woodruff T.J. *Sec A*, 84, 170-180.
- Jelen et al., 2012 – Jelen H.H., Majcher M., et M Dziadas. *Analitica Chimica Acta*, 738, 13-26.
- Hays et al., 2003 – Hays S.M., Aylward L.L. *Toxicol, Pharmacol*, 37, 202-217.
- Tanabe et al., 1993 – Iwata H., Tanabe S., Sakai N., Tatsukawa R. *Environ. Sci. Technol.* 27, 1080-1098.
- Kirrluk et al., 1995 – Kirrluk R.M., Servos M.R., White D.M., Cabana G., Rasmussen J.B. *Sci.* 52, 2660-2674.
- Kosikowska et al., 2010 – Kosikowska M., Biziuk M. *Chem*, 29, 1064-1072.
- Svjetlana et al., 2010 – Rada D.D., Jelena S.G.U., Svjetlana B.C., Ljubiša M.I. *Soc*, 21, 985-994.
- Raposo et al., 2007 – Raposo J.J.L., Ré-Poppi N. *Talanta* 72, 1833-1841.
- Rianawati et al., 2009 – Rianawati E., Balasubramanian R. *Physics and Chemistry of the Earth*, 34, 857-865.
- Mesquita et al., 2011 – Rodrigues F.M., Mesquita P.R.R., Oliveira S.L., Oliveira F.S., Filho A.M., Pereira P.A., Andrade J. B. *Microchemical Journal*, 98, 56-61.
- Vidal et al., 2009 – J.L.M. Vidal, P. Plaza-Bolanos, R. Romero-Gonzalez., A.G Frenich, *J. Chromato A*, 40, 6767-6788.
- Shahsavand et al., 2018 – Shahsavand H., Nateghi M.R. *Journal of Water Chemistry and Technology*, 86-90.
- Anandhakumar et al., 2013 – Anandhakumar S., Mathiyarasu J., Phani K.L.N. *Analyst*. 138, 5674-5678.

Copyright © 2018 by Academic Publishing House Researcher s.r.o.



Published in the Slovak Republic  
European Reviews of Chemical Research  
Has been issued since 2014.  
E-ISSN: 2413-7243  
2018, 5(2): 75-85

DOI: 10.13187/erchr.2018.2.75  
[www.ejournal14.com](http://www.ejournal14.com)



## Synthesis and Visible Spectra Studies of Novel Pyrazolo/Oxazole Merocyanine Dyes

H.A. Shindy <sup>a,\*</sup>, M.A. El-Maghraby <sup>a</sup>, M.M. Goma <sup>a</sup>, N.A. Harb <sup>a</sup>

<sup>a</sup> Department of Chemistry, Faculty of Science, Aswan University, Aswan 81528, Egypt

### Abstract

Novel acyclic merocyanine dyes and cyclic merocyanine dyes derived from the nucleus of furo[(3,2-d)pyrazole;(3',2'-d)oxazole] were prepared. The electronic visible absorption spectra of all the new synthesized acyclic and cyclic merocyanine dyes were examined in 95 % ethanol solution to evaluate their spectral sensitization properties. Studying the electronic visible absorption spectra of cyanine dyes in 95 % ethanol solution have a great practical value and is very important study in the case of cyanine dyes because the extensive uses and applications of these dyes as photographic sensitizers for silver halide emulsion in photosensitive material industry for coloured and non coloured (black and white) films (cyanine dyes were originally used, and still are, to increase the sensitivity range of photographic emulsions, i.e. to increase the range of wavelengths which will form an image on the film). Structural characterization and identification was carried out via elemental analysis, visible spectra, mass, IR and <sup>1</sup>H NMR spectroscopic data.

**Keywords:** cyanine dyes, merocyanine dyes, synthesis, visible absorption spectra, acyclic merocyanine, cyclic merocyanine.

### 1. Introduction

Merocyanine dyes (Shindy et al., 2012; Shindy et al., 2016; Shindy et al., 2008) have found wide application in various areas of science and technology. They are used as optical sensors, spectral sensitizers for silver halide photography (Peng et al., 1996; Chen et al., 1995; Araki et al., 1997), and recording medium in optical disks. Their potential application as photosensitizers for photodynamic therapy (PDT) (Gomer et al., 1991; Krieg et al., 1993; Redmond et al., 1994) and radiation sensitizers for solid tumor treatment (Harriman et al., 1991) has been extensively studied. Merocyanine dyes are promising materials for future technological applications, including nonlinear optics, solar and hydrogen energy, laser technology, and nanotechnology.

In addition, it is worthy of special attention that merocyanines (often called photomerocyanines) are obtained during the UV irradiation or heating of spiropyrans (Bertelson, 1999; Minkin, 2004; Lukyanov, Lukyanova, 2005). Their photo- and thermochromic properties are of considerable interest, and spiropyrans have been proposed for optical memory and switches (Berkovic, et al., 2000), metal ions extraction (Alfimov et al., 2003; Kimura et al., 2004), photocontrollable ferromagnetics (Taguchi et al., 2003; Kashima et al., 2005), and optical and fluorescence sensors on metal ions and biological objects (Evans et al., 1993; Voloshin et al., 2004; Tomizaki et al., 2005).

\* Corresponding author

E-mail addresses: [hashindy2@hotmail.com](mailto:hashindy2@hotmail.com) (H.A. Shindy)

Besides, merocyanine dyes are heterocyclic chromophores that are extensively used in a number of areas (i.e., as photographic sensitizers, for nonlinear optics, and in chemotherapy) (Chen et al., 2006; Yow et al., 2000; Zareba et al., 2005; Marder, 2006; Marder et al., 1993; Brooker et al., 1951). Recently they have also been employed as sensors of protein conformation and protein interactions in live cell imaging (Nalbant et al., 2004). The efficacy of merocyanine dyes as components of biosensors depends not only on their fluorescence emission properties, but also not their photostability.

In this research paper we prepared novel series of acyclic and cyclic merocyanine dyes as new synthesis contribution and spectroscopic investigation in the field, and to may be used and/or applied in any of the wide uses and applications of cyanine dyes, and particularly as photographic sensitizers in photographic material industry, as indicators in operations of acid-base titration in analytical chemistry, as probes for determining solvent polarity in physical, physical organic and/or in inorganic chemistry and as bactericidal and fungicidal in pharmaceutical (pharmacological) industry and/or in pharmacology.

## 2. Results and discussion

### 2.1. Synthesis

Oxidation of the compound 3,5-dimethyl-7-phenyl-furo[(3,2-d)pyrazole;(3',2'-d)oxazole] (1) with bimolar ratios of selenium dioxide, yielded the compound 3,5-dicarbonyl-7-phenyl-furo[(3,2-d)pyrazole;(3',2'-d)oxazole] (2), Scheme (1).

Subsequent reaction of the diformyl compound (2) with equimolar or bimolar ratios of acyl and/or acyl derivatives (acetaldehyde, acetone, acetophenone, p-methoxyacetophenone, or p-nitroacetophenone) in ethanol as organic solvent containing piperidine as a basic catalyst resulted the acyclic merocyanine dyes (3a-e) or bis acyclic merocyanines (4a-e). See Scheme (1), Route (1).

Chemical confirmations for the bis acyclic merocyanine dyes (4a-e) were carried out through, Route (2), via reactions of the previously prepared acyclic merocyanine dyes (3a-e) with equimolar ratios of the acyl and/or acyl derivatives (acetaldehyde, acetone, acetophenone, p-methoxyacetophenone, p-nitroacetophenone) in ethanol containing few drops of piperidine to achieve the same bis acyclic merocyanine dyes (4a-e) obtained through Route 1, characterized by the same melting points, mixed melting points, the same visible, IR and <sup>1</sup>H-NMR spectra. Scheme (1).

In addition, the diformyl compound (2) was reacted with equimolar or bimolar ratios of acetylacetone or ethylacetoacetate in ethanol as solvent containing piperidine as basic catalyst and resulted the acyclic merocyanine dyes (5a, b) or bis acyclic merocyanines (6a, b). See Scheme (1), Route (1).

Chemical confirmations for the bis acyclic merocyanine dyes (6a, b) were carried out through, Route (2), via reactions of the previously prepared acyclic merocyanine dyes (5a, b) with equimolar ratios of acetylacetone or ethylacetoacetate in ethanol and presence of piperidine to achieve the same bis acyclic merocyanine dyes (6a, b) obtained through Route (1), characterized by the same melting points, mixed melting points, the same visible, IR and <sup>1</sup>H-NMR spectra, Scheme (1).

Besides, an equimolar and/or bimolar ratios of hydantoin (imidazolid-2, 4-dione) were reacted with the diformyl compound (2) in ethanol as organic solvent containing piperidine as a basic catalyst and achieved cyclic merocyanine or bis cyclic merocyanine dyes (7) and (8) respectively, Scheme (1).

Chemical confirmations were carried out through the reaction of the previously prepared cyclic merocyanine dye (7) and equimolar ratios of hydantoin in ethanol and presence of piperidine through Route (2), to achieve the same bis cyclic merocyanine dye (8) obtained through Route (1), characterized by the same melting points, mixed melting points, the same visible, IR and <sup>1</sup>H-NMR spectra, Scheme (1).

The structures of the prepared compounds was characterized and identified by elemental analysis, Tables (1), (2) and (3) visible spectra, Tables 1, 2 and 3, Mass spectrometer, IR (Wade, 1999) and <sup>1</sup>H NMR (Wade, 1999a) spectroscopy, Table 4.

### 2.2. Visible spectra studies

The electronic visible absorption spectra of the acyclic merocyanine dyes (3a-e) and the bis acyclic merocyanine dyes (4a-e) in 95 % ethanol solution reveal bands in the visible region 440-620 nm and 390-630 nm, respectively. The positions of these bands underwent displacements to give

bathochromic shifts and/or hypsochromic shifts accompanied by increasing and / or decreasing the intensity of the bands depending upon the type of the side chain substituent (R), Tables (1) and (2).

So, substituting R = H in the acyclic (bis acyclic) merocyanine dyes 3a (4a) by R = CH<sub>3</sub> to give dyes 3b (4b) caused bathochromic shifts for the absorption band by 10 nm in addition to increasing the intensity of the bands, Tables (1) and (2). This can be attributed to the electron donating character of the CH<sub>3</sub> group in the latter dyes 3b (4b) which facilitate and increases the strength and intensity of the electronic charge transfer to the positive center of the carbonyl group and consequently red shifts occurs in correspondence to the H atom in the former dyes 3a (4a).

In addition, substituting R = H by R = ph moving from dyes 3a (4a) to dyes 3c (4c) resulted in a red shifts by 20 nm accompanied with increasing the intensity of the absorption bands, Tables 1 and 2. This can be related to increasing  $\pi$ -delocalization conjugation in the latter dyes 3c (4c) due to the presence of additionally phenyl ring system.

Besides, substituting R = ph in the dyes 3c (4c) by R = C<sub>6</sub>H<sub>5</sub>-p.OCH<sub>3</sub> and / or C<sub>6</sub>H<sub>4</sub>-p.NO<sub>2</sub> to give dyes 3d (4d) and / or 3e (4e) makes bathochromic and / or hypsochromic shifts for the absorption bands by 10 nm and / or 30 nm, accompanied by quenching the intensity of the bands, respectively, Tables (1) and (2). This can be related to the electron releasing character of the methoxy group in dyes 3d (4d) and / or the electron attracting character of the NO<sub>2</sub> group in the dyes 3e (4e). Electron releasing groups increase the strength of the intensity of electronic charge transfer from the basic center of the dye (oxygen atom and / or nitrogen atom) to the acidic center of the dye (polarized carbonyl group) and consequently red shifts occurs. Electron attracting groups decreases the strength of the intensity of electronic charge transfer pathways from the basic center of the dye (oxygen atom and/or nitrogen atom) to the polarized acidic center of the dye (carbonyl group), and accordingly blue shift occurs, Scheme (2).

Comparing the electronic visible absorption spectra of the acyclic merocyanine dyes (3a-e) with those of the bis acyclic merocyanine dyes (4a-e) declared that the latter dyes have bathochromically shifted bands related to the former ones, Tables 1 and 2. This can be attributed to the presence of two factors. The first factor is the presence of two electronic charge transfer pathways inside the latter dyes molecules in correspondance to one electronic charge transfer pathways inside the former dyes molecules, Scheme (2). The second factor is increasing conjugation due to increasing the number of methine units in bis acyclic merocyanine dyes (4a-e) related to the former acyclic merocyanine dyes (3a-e) by two methine unit. Scheme (1).

Additionally, the electronic visible absorption spectra of the acyclic (bis acyclic) merocyanine dyes 5a, b (6a, b) and cyclic (bis cyclic) merocyanine dyes 7 (8) disclose bands in the visible region 420-590 nm (440-600 nm) and 600-610 nm respectively. The positions of these bands and their molar extinction coefficients are influenced by the kind of R substituted in the dyes 5a, b (6a, b) molecules and by the cyclic ring system in dyes 7 (8), Table (3). So, substituting R = COOEt by R = COCH<sub>3</sub> transferring from dyes 5a (6a) to dyes 5b (6b) makes a remarkable bathochromic shifts for the absorption bands by 10 nm. This can be related to the strong powerful electron pulling character of the ethoxy group in the former dyes 5a (6a) in correspondence to the strong electron pushing character of the methyl group in the latter dyes 5b (6b).

Furthermore, comparing the electronic visible absorption spectra of the acyclic merocyanine dyes 5a, b (6a, b) with those of the cyclic merocyanine dyes 7 (8) showed that the latter cyclic merocyanine dyes 7 (8) reveals bathochromic shifted band by 10 nm and 20 nm in addition to increasing the intensity of the bands, Table 3. This may be attributed to the presence of two basic center (two nitrogen atoms) in the cyclic ring system of the latter dyes 7 (8), which facilitate and increase the intensity of electronic charge transfer pathways to the acidic center of the dyes (positively polarized carbonyl group) and consequently red shifts occurs.

Comparing the electronic visible absorption spectra of the acyclic merocyanine dyes (5a, b) with those of the bis acyclic merocyanine dyes (6a, b) declared that the latter dyes have bathochromically shifted bands related to the former ones, Table 3. This can be attributed to the presence of two factors. The first factor is the presence of two electronic charge transfer pathways inside the latter dyes molecules in correspondance to one electronic charge transfer pathways inside the former dyes molecules, Scheme (2). The second factor is increasing conjugation due to increasing the number of methine units in bis acyclic merocyanine dyes (6a, b) related to the former acyclic merocyanine dyes (5a, b) by two methine unit, Scheme (1).

Comparing the electronic visible absorption spectra of the cyclic merocyanine dye (7) with those of the bis cyclic merocyanine dye (8) declared that the latter dye has bathochromically shifted bands related to the former one. This can be attributed to the presence of two factors. The first factor is the presence of two electronic charge transfer pathways inside the latter dye molecule in correspondance to one electronic charge transfer pathways inside the former dye molecule, Scheme (2). The second factor is increasing conjugation due to increasing the number of methine units in bis cyclic merocyanine dye (8) related to the former cyclic merocyanine dye (7) by one methine unit, Scheme (1).

### 3. Conclusion

From the above discussed results we could conclude that:

1. The electronic visible absorption spectra of the synthesized acyclic (3a-e), (4a, b), bis acyclic (5a-e), (6a, b), cyclic (7) and bis cyclic (8) merocyanine dyes in 95 % ethanol solution underwent displacements to give bathochromic shifted and/or hypsochromic shifted bands accompanied by increasing and/or decreasing the intensity of the absorption bands depending upon the following factors:

a. Presence of electron donating and / or electron attracting groups in the dyes molecules in the order of: electron donating group dyes > electron attracting group dyes.

b. Increasing  $\pi$ -delocalization conjugations in the dyes molecules in the order of: Ph dyes > H dyes.

c. Increasing the number of the basic centers inside the dyes molecules, in the order of: Hydantoin dyes > COOEt, COCH<sub>3</sub> dyes

d. Increasing and / or decreasing the number of the electronic charge transfer pathways inside the dyes molecules in the order of: two electronic charge transfer pathways dyes > one electronic charge transfer pathways dyes.

e. Increasing and/or decreasing conjugation due to increasing and/or decreasing number of the methine units inside the dyes structure, in the order of: more methine units dyes > less methine units dyes.

2. The intensity of the colour of the synthesized acyclic (bis acyclic) and cyclic (bis cyclic) merocyanine dyes can be related to suggested two mesomeric electronic transitions structures (A) and (B) producing a delocalized positive charge over the conjugated chromophoric group system of the dyes, Scheme (2).

### 4. Experimental

#### 4.1. General

All the melting points of the prepared compounds are measured using Electrothermal 15V, 45W 1 A9100 melting point apparatus (Chemistry Department, Faculty of Science, Aswan University, Aswan, Egypt) and are uncorrected. Elemental analysis was carried out at the Microanalytical Center of Cairo University by an automatic analyzer (Vario EL III Germany). Infrared spectra were measured with a FT-IR (4100 Jasco, Japan), Cairo University. <sup>1</sup>HNMR spectra were accomplished using Varian Gemini-300 MHz NMR Spectrometer (Cairo University). Mass Spectroscopy was recorded on Mass 1: GC2010 Shimadzu Spectrometer (Cairo University). Electronic visible absorption spectra were carried out on vis spectrophotometer spectra 24 RS Labomed, INC. (Chemistry Department, Faculty of Science, Aswan University, Aswan, Egypt).

#### 4.2. Synthesis

##### 4.2-1. Synthesis of 3,5-dicarbaldehyde-7-phenyl-furo[(3,2-d)pyrazole;(3',2'-d)oxazole] (2):

A mixture of 1:2 molar ratios of the compound (1), (0.01 mol, 0.25 gm) and selenium dioxide (0.02 mol, 0.22 gm) were dissolved in dioxane (50 ml). The reaction mixture was heated under reflux for 16 hrs. It was filtered off while hot to remove Selenium metal, concentrated, cooled, and then precipitated by adding cold water. The precipitated product was filtered, air dried, collected, and then recrystallized from ethanol. The data are shown in Table (1).

##### 4.2-2. Synthesis of 5-carbaldehyde-7-phenyl-furo[(3,2-d)pyrazole; (3',2'-d)oxazole-3(1)-acyclic merocyanine dyes (3a-e):

A mixture of equimolar ratios (0.01 mol) of acetaldehyde (0.06 gm), acetone (0.07 gm), acetophenone (0.12 gm), p-methoxyacetophenone (0.15 gm), or p-nitroacetophenone (0.17 gm) and the dicarbaldehyde compound (2) (0.28 gm) was dissolved in ethanol (50 ml) containing piperidine (1-2 ml). The reaction mixture, was boiled under reflux for 6 hrs. and its colour changed from reddish colour to deep brown colour at the end of the refluxing time. It was filtered while hot to remove any impurities, concentrated, cooled and precipitated by adding ice-water mixture to give the acyclic merocyanine dyes (3a-e) which crystallized from ethanol. The data were given in Table (1).

#### 4.2-3. Synthesis of 7-phenyl-furo[(3,2-d)pyrazole;(3',2'-d)oxazole-3,5(1)-bis acyclic merocyanine dyes (4a-e):

Two different methods were used to prepare these cyanine dyes:

**Method (1):** A mixture of bimolar ratios (0.02 mol) of acetaldehyde (0.12 gm), acetone (0.14 gm), acetophenone (0.24 gm), p-methoxyacetophenone (0.3 gm), or p-nitroacetophenone (0.33 gm) and the diformyl compound (2) (0.01 mol, 0.28 gm) were refluxed for 6 hrs in ethanol (50 ml) containing piperidine (1 ml). The reaction mixture, which changed from brown colour to deep brown colour at the end of refluxing, was filtered while hot to remove any impurities, concentrated, cooled, neutralized with acetic acid and precipitated by adding cold water to give the bis acyclic merocyanine dyes (4a-e) which was crystallized from ethanol. The data are given in Table (2).

**Method (2):** A mixture of equimolar ratios (0.01 mol) of acetaldehyde (0.06 gm), acetone (0.07 gm), acetophenone (0.12 gm), p-methoxyacetophenone (0.15 gm), or p-nitroacetophenone (0.17 gm) and the previously prepared cyclic merocyanine dyes (3a-e) (0.01 mol) (0.33 gm for 3a, 0.36 gm for 3b, 0.49 gm for 3c, 0.55 gm for 3d, 0.58 gm for 3e) were refluxed for 6 hrs in ethanol (50 ml) containing piperidine (1 ml) as a catalyst. The reacting materials were attained a permanent intense brown colour at the end of the refluxing time. It was filtered off while hot, concentrated, cooled, precipitated by adding cold water. The precipitates were collected and recrystallized from ethanol to give the same bis cyclic merocyanine dyes obtained by route (1), characterized by melting points, mixed melting points, same visible, IR and <sup>1</sup>H-NMR spectral data, Table (2).

#### 4.2-4. Synthesis of 5-carbaldehyde-7-phenyl-furo[(3,2-d)pyrazole; (3',2'-d)oxazole-3[2(3)] acyclic merocyanine dyes (5a, b):

An equimolar ratios (0.01 mol) of ethylacetoacetate (0.13 gm) or acetylacetone (0.1 gm) and the 3,5-dicarbaldehyde compound (2) (0.28 gm) were heated under reflux for 6 hrs in ethanol (50 ml) containing piperidine (1-2 ml). The reaction mixture, which changed from red colour to deep brown colour at the end of refluxing, was filtered while hot to remove any impurities, concentrated, cooled, precipitated by adding cold water. The precipitates were filtered off, dried and crystallized from ethanol to give the acyclic merocyanine dyes (5a, b). The data are listed in Table 3.

#### 4.2-5. Synthesis of 7-phenyl-furo[(3,2-d)pyrazole;(3',2'-d)oxazole-3,5[2(3)]-bis acyclic merocyanine dyes (6a, b):

Two different methods were used to prepare these cyanines:

**Method (1):** A mixture of bimolar ratios (0.02 mol) of ethylacetoacetate (0.25 gm) and acetylacetone (0.2 gm) and unimolar ratios of the diformyl compound (2) (0.01 mol, 0.28 gm) was refluxed for 6 hrs in ethanol (50 ml) as solvent containing piperidine (1 ml) as a catalyst. The reaction mixture, which changed from brown colour to deep brown colour at the end of refluxing, was filtered while hot to remove any impurities, concentrated, cooled, neutralized with acetic acid and precipitated by adding cold water to give the bis acyclic merocyanine dyes (6a, b) which was crystallized from ethanol. The data are given in Table 3.

**Method (2):** A mixture of equimolar ratios (0.01 mol) of either ethylacetoacetate (0.13 gm) or acetylacetone (0.1 gm) and the previously prepared acyclic merocyanine dyes (5a, b) (0.01 mol) (0.39 gm for 5a, 0.36 gm for 5b) were refluxed for 6 hrs in ethanol (50 ml) containing piperidine (1 ml) as catalyst. The reacting materials were attained a permanent intense brown colour at the end of the refluxing time. It was filtered off while hot, concentrated, cooled, and precipitated by adding water. The precipitates were collected and recrystallized from ethanol to give the same bis cyclic merocyanine dyes obtained by route (1), characterized by melting points, mixed melting points, same visible, IR and <sup>1</sup>H-NMR spectral data, Table 3.

#### 4.2-6. Synthesis of 5-carbaldehyde-7-phenyl-furo[(2,3-d)pyrazole;(3',2'-d)oxazole-3(4)-cyclic merocyanine dye (7):

Equimolar ratios of hydantoin (0.01 mol, 0.11 gm) and the diformyl compound (2) (0.01 mol, 0.3 gm) were heated under reflux in ethanol (50 ml) and presence of piperidine (1-2 ml) for 6 hrs and attained deep brown colour at the end of refluxing. The reaction mixture was filtered off on hot, concentrated, cooled, and precipitated by adding ice-water mixture. The separated cyclic merocyanine dye (7) was filtered off, washed with water, dried and crystallized from ethanol. The data were recorded in [Table 3](#).

#### 4.2-7. Synthesis of 7-phenyl-furo[(3,2-d)pyrazole;(3',2'-d)oxazole-3, 5(4)-bis cyclic merocyanine dye (8):

Two different methods were used to prepare these cyanine dyes:

**Method (1):** Bimolar ratios of hydantoin (0.02 mol, 0.2 gm) were heated under reflux with unimolar ratios of the diformyl compound (2) (0.01 mol, 0.3 gm) in ethanol (50 ml) and presence of piperidine (1 ml) for 6 hrs. The reaction mixture attained reddish violet permanent colour at the end of the refluxing time. It was filtered off on hot, concentrated, cooled, neutralized with glacial acetic acid and precipitated by adding ice-water mixture. The separated bis cyclic merocyanine dye (8) was filtered, washed with water, dried and recrystallized from ethanol. The results are listed in [Table 3](#).

**Method (2):** A mixture of equimolar ratios of hydantoin (0.01 mol) (0.11 gm) and the previously prepared cyclic merocyanine dye (7) (0.01 mol) (0.36 gm) was boiled under reflux for 6 hrs in ethanol (50 ml) containing piperidine (1 ml) as a catalyst. The reacting materials were attained a permanent intense brown colour at the end of the refluxing time. It was filtered off while hot, concentrated, cooled and precipitated by adding cold water. The precipitates were collected and recrystallized from ethanol to give the same bis cyclic merocyanine dyes obtained by route (1), characterized by melting points, mixed melting points, same visible, IR and <sup>1</sup>H-NMR spectral data, [Table 3](#).

#### 4.3. Visible spectra studies

The electronic visible absorption spectra of the prepared cyanine dyes were examined in 95 % ethanol solution and recorded using 1Cm Qz cell in visible spectrophotometer, spectro 24 RS Labomed, INC. A stock solution (1x10<sup>-3</sup>M) of the dyes was prepared and diluted to a suitable volume in order to obtain the desired lower concentrations. The spectra were recorded immediately to eliminate as much as possible the effect of time.

### 5. Conflict of interest

There is no conflict of interest.

### 6. Acknowledgement

We are thankful to the Chemistry department, Faculty of Science, Aswan University, Aswan, Egypt for supporting this work.

### References

- [Shindy et al., 2012](#) – Shindy, H.A., El-Maghraby, M.A. and Eissa, F.M. (2012). *Dyes and Pigments*, 92 (3), 929-935.
- [Shindy et al., 2016](#) – Shindy, H.A., Khalafalla, A.K., Goma, M.M., Eed, A.H. (2016). *Chemistry International*, 2 (3), 114-120.
- [Shindy, et al., 2008](#) – Shindy, H.A., El-Maghraby, M.A., Eissa, F.M. (2008). *Coloration Technology*, 124 (3), 159-164.
- [Peng et al., 1996](#) – Peng, Z., Zhou, X., Carroll, S., Geise, H. J., Peng, B., Dommissie, R., Esmansc, E., Carleer, R. (1996). *J. Mater. Chem.* 6: 1325.
- [Chen, et al. 1995](#) – Chen, C., Zhou, B., Lu, D., Xu, G. (1995). *J. Photogr. Sci.* 43: 134.
- [Araki, et al., 1997](#) – Araki, T., Ito, E., Oichi, K., Mitsumoto, R., Sei, M., Oji, H., Yamamoto, Y., Ouchi, Y., Seki, K., Takata, Y., Edamatsu, K., Yokoyama, T., Ohta, T., Kitajima, Y., Watanabe, S., Yamashita, K., Tani, T. (1997). *J. Phys. Chem. B* 101: 10378.
- [Gomer, et al., 1991](#) – Gomer, C. (1991). *Photochem. Photobiol.*, 54:1093.
- [Krieg et al., 1993](#) – Krieg, M., Redmond, R.W. (1993). *Photochem Photobiol.*, 57: 472.
- [Redmond et al., 1994](#) – Redmond, R.W., Srichai, M.B., Bilitz, J.M., Schlomer, D.D., Krieg, M. (1994). *Photochem Photobiol.*, 60: 348.

- Harriman et al., 1991 – Harriman, A.L., Shoute, C.T., Neta, P. (1991). *J. Phys. Chem.*, 95:2415.
- Bertelson, 1999 – Bertelson, R.C. (1999). Spiropyran. In: Crano JS, Guglielmetti R (eds). *Organic Photo-chromic and Thermo-chromic Compounds*. Plenum Press, New York, p. 11.
- Minkin, 2004 – Minkin, V.I. (2004). *Chem. Rev.*, 104: 2751.
- Lukyanov, Lukyanova, 2005 – Lukyanov, B.S., Lukyanova, M.B. (2005). *Chem. Heterocycl. Comp.* 41: 281.
- Berkovic et al., 2000 – Berkovic, G., Krongauz, V., Weiss, V. (2000). *Chem. Rev* 100: 1741.
- Alfimov et al., 2003 – Alfimov, M.V., Fedorova, O.A., Gromov, S.P. (2003). *J. Photochem. Photobiol. A* 158: 183.
- Kimura et al., 2004 – Kimura, K., Sakamoto, H., Uda, R.M. (2004). *Macromolecules*, 37: 1871.
- Taguchi et al., 2003 – Taguchi, M., Li, G., zh, Gu., Sato, O., Einada, Y. (2003). *Chem Mater.*, 15: 4756.
- Kashima, et al., 2005 – Kashima, I., Okubo, M., Qno, Y., Itoi, M., Kida, N., Hikita, M., Enomoto, M., Kojima, N. (2005). *Synth Metals.*, 155: 703.
- Evans, et al., 1999 – Evans, III.L., Collins, G.E., Shaffer, R.E., Michelet, V., Winkler, J.D. (1999). *Anal. Chem.*, 71: 5322.
- Voloshin, et al., 2004 – Voloshin, N.A., Chernyshev, A.V., Metelitsa, A.V., Besugliy, S.O., Voloshina, E.N., Sadimenko, L.P., Minkin, V.I. (2004). *Arkhivoc*, 11: 16.
- Tomizaki, et al., 2005 – Tomizaki, K., Jieb, X., Mihara, H. (2005). *Bioorg. Med Chem. Lett.*, 15: 1731.
- Chen et al., 2006 – Chen, J., Mak, N. K., Leung, W., Cheung, N., Peng, Q. (2006). *J. Environ. Pathol. Toxicol. Oncol.*, 25, 217-222.
- Yow, et al., 2000 – Yow, C.M., Mak, N.K., Szeto, S., Chen, J.Y., Lee, Y.L., Cheung, N.H., Huang, D.P., Leung, A.W. (2000). *Toxicol. Lett.*, 115, 53-61.
- Zareba, et al., 2005 – Zareba, M., Niziolek, M., Korytowski, W., Girotti, A.W. (2005). *Biochem. Biophys. Acta*, 1722, 51-59.
- Marder, 2006 – Marder, S.R. (2006). *Chem. Commun.*, 131-134.
- Marder et al., 1993 – Marder, S. R., Gorman, C.B., Tiemann, B.G., Cheng, L.T. (1993). *J. Am. Chem. Soc.*, 115, 3006-3007.
- Brooker, et al., 1951 – Brooker, L.G.S., Keyes, G.H., Sprague, R.H., VanDyke, R.H., Vanlare, E., VanZandt, G., White, F.L.; Cressman, H.W.J.; Dent, S.G. (1951). *J. Am. Chem. Soc.*, 73, 5332-5350.
- Nalbant, et al., 2004 – Nalbant, P., Hodgson, L., Kraynov, V., Toutchkine, A., Hahn, K.M. (2004). *Science*. 305, 1615-1619.
- Wade, 1999 – Wade Jr., L.G. (1999). *Organic Chemistry.*, 4th Edn., Pearson Educ. (Prentice Hall, Upper Saddle River, New Jersey 07458, USA), 500-538.
- Wade, 1999a – Wade Jr., L.G. (1999). *Organic Chemistry.*, 4th Edn., Pearson Educ. (Prentice Hall, Upper Saddle River, New Jersey 07458, USA), 544-560.

## Appendix

Table 1: Characterization of the prepared compounds 2, (3a-e).

Comp No.	Nature of products			Molecular formula (M.Wt)	Analysis%						Absorption spectra in 95% ethanol	
	Colour	yield %	MP C°		Calculated			Found			$\lambda_{\max}$ (nm)	$\epsilon_{\max}$ (mol <sup>-1</sup> .cm <sup>2</sup> )
					C	H	N	C	H	N		
2	Deep reddish brown	50	110	C <sub>14</sub> H <sub>7</sub> N <sub>3</sub> O <sub>4</sub> (281)	59.79	2.49	14.95	59.77	2.45	14.91	.....	.....
3a	Deep violet	41	145	C <sub>16</sub> H <sub>9</sub> N <sub>3</sub> O <sub>4</sub> (307)	62.54	2.93	13.68	62.52	2.9	13.63	440, 460, 590	9570, 10330, 5620
3b	Deep violet	45	130	C <sub>17</sub> H <sub>11</sub> N <sub>3</sub> O <sub>4</sub> (321)	63.55	3.43	13.08	63.53	3.42	13.02	390, 470, 600	15420, 8780, 4860
3c	Deep violet	43	155	C <sub>22</sub> H <sub>13</sub> N <sub>3</sub> O <sub>4</sub> (383)	68.93	3.39	10.97	68.91	3.35	10.95	400, 450, 480, 510, 610	15030, 8540, 9320, 8470, 5050
3d	Deep violet	47	120	C <sub>23</sub> H <sub>15</sub> N <sub>3</sub> O <sub>5</sub> (413)	66.83	3.63	10.17	66.79	3.61	10.13	470, 490, 530, 620	8340, 9920, 7740, 5230
3e	Deep violet	42	125	C <sub>22</sub> H <sub>12</sub> N <sub>4</sub> O <sub>6</sub> (428)	61.68	2.8	13.08	61.65	2.77	13.03	450, 500, 580	9340, 7180, 5120

Table 2: Characterization of the prepared compounds (4a-e).

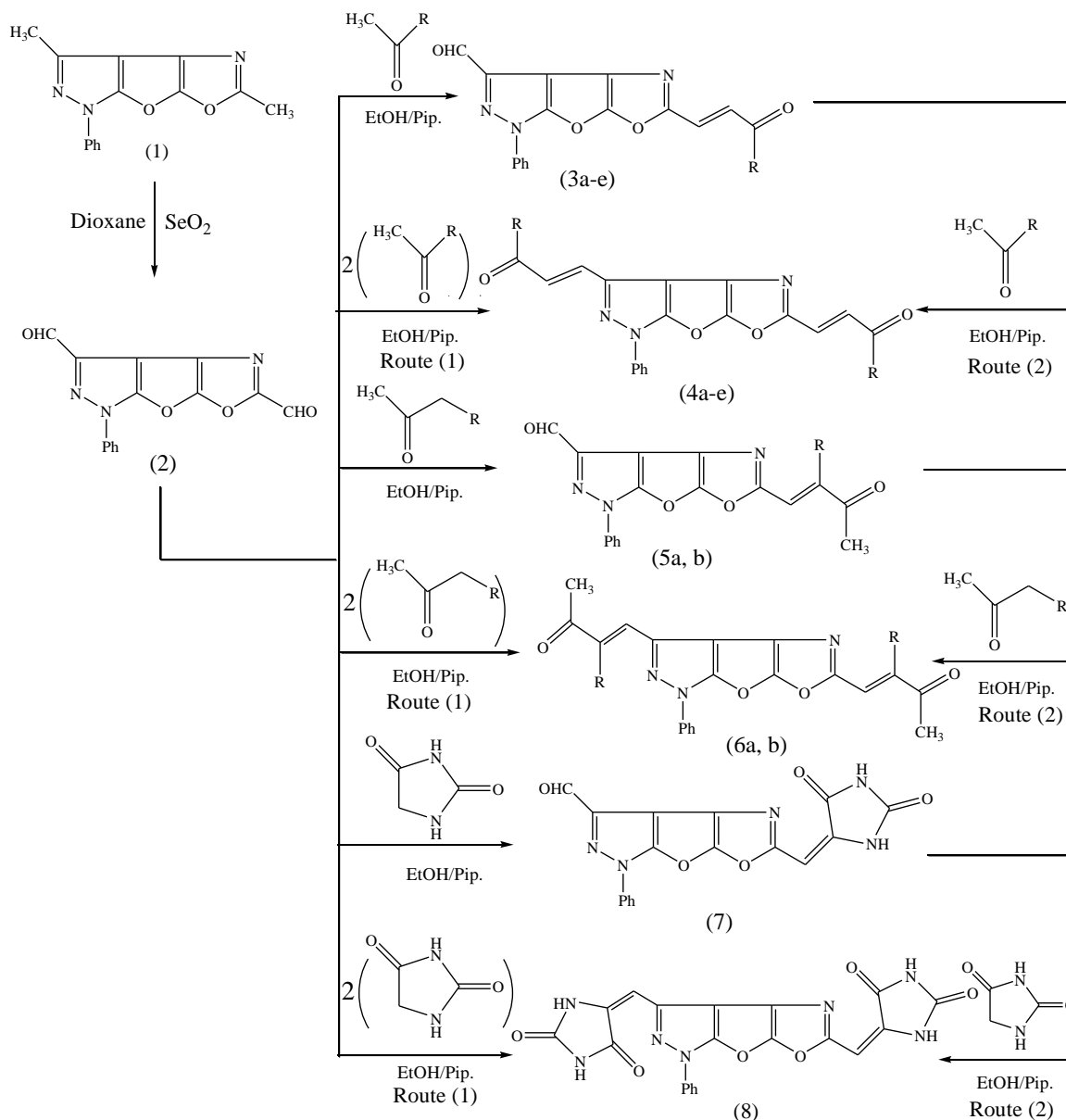
Comp No.	Nature of products			Molecular formula (M.Wt)	Analysis%						Absorption spectra in 95% ethanol	
	Colour	yield %	MP C°		Calculated			Found			$\lambda_{\max}$ (nm)	$\epsilon_{\max}$ (mol <sup>-1</sup> .cm <sup>2</sup> )
					C	H	N	C	H	N		
4a	Deep violet	46	115	C <sub>18</sub> H <sub>11</sub> N <sub>3</sub> O <sub>4</sub> (333)	64.86	3.3	12.61	64.81	3.28	12.59	390, 450, 470, 600	15200, 9050, 9700, 4660
4b	Deep violet	44	150	C <sub>20</sub> H <sub>15</sub> N <sub>3</sub> O <sub>4</sub> (361)	66.48	4.16	11.63	66.45	4.12	11.61	470, 520, 610	9700, 8490, 4990
4c	Deep violet	48	140	C <sub>30</sub> H <sub>19</sub> N <sub>3</sub> O <sub>4</sub> (485)	74.23	3.92	8.66	74.21	3.89	8.62	490, 530, 620	9850, 8480, 5160
4d	Deep violet	45	160	C <sub>32</sub> H <sub>23</sub> N <sub>3</sub> O <sub>6</sub> (545)	70.46	4.22	7.71	70.44	4.19	7.68	500, 540, 630	9890, .7780, 5390
4e	Deep violet	43	135	C <sub>30</sub> H <sub>17</sub> N <sub>5</sub> O <sub>8</sub> (575)	62.61	2.96	12.17	62.58	2.94	12.13	440, 460, 490, 590	8150, 9530, 8000, 5030

Table 3: Characterization of the prepared compounds (5a, b), (6a, b), 7 and 8.

Comp No.	Nature of products			Molecular formula (M.Wt)	Analysis%						Absorption spectra in 95% ethanol	
	Colour	yield %	MP C°		Calculated			Found			$\lambda_{\max}$ (nm)	$\epsilon_{\max}$ (mol <sup>-1</sup> .cm <sup>2</sup> )
					C	H	N	C	H	N		
5a	Reddish violet	56	135	C <sub>20</sub> H <sub>15</sub> N <sub>3</sub> O <sub>6</sub> (393)	61.07	3.82	10.69	61.03	3.8	10.65	420, 440, 480, 580	7720, 10370, 7750, 5530
5b	Reddish violet	59	150	C <sub>19</sub> H <sub>13</sub> N <sub>3</sub> O <sub>5</sub> (363)	62.81	3.58	11.57	62.79	3.55	11.52	430, 460, 490, 590	9490, 10530, 8850, 5340
6a	Reddish violet	57	140	C <sub>26</sub> H <sub>23</sub> N <sub>3</sub> O <sub>6</sub> (505)	61.78	4.55	8.32	61.73	4.51	8.31	440, 490, 590	9720, 7940, 5210
6b	Reddish violet	60	155	C <sub>24</sub> H <sub>19</sub> N <sub>3</sub> O <sub>6</sub> (445)	64.72	4.27	9.44	64.71	4.22	9.41	430, 460, 500, 600	8340, 9520, 7800, 4900
7	Reddish violet	62	160	C <sub>17</sub> H <sub>9</sub> N <sub>5</sub> O <sub>5</sub> (363)	56.2	2.48	19.28	56.18	2.45	19.24	450, 470, 500, 600	7200, 8700, 7700, 5080
8	Reddish violet	64	170	C <sub>20</sub> H <sub>11</sub> N <sub>7</sub> O <sub>6</sub> (445)	53.93	2.47	22.02	53.91	2.44	22.01	450, 480, 510, 610	135

**Table 4.** IR and <sup>1</sup>H NMR (Mass) Spectral Data of the Prepared Compounds (2), (3a), (4a), (5b), (6b), (7) and (8)

Comp. No.	IR Spectrum (KBr, Cm <sup>-1</sup> )	<sup>1</sup> H NMR Spectrum (DMSO, δ); & (Mass data).
2	699, 748 (monosubstituted phenyl). 1031, 1116, 1170 (C—O—C cyclic). 1301, 1362 (C—N). 1493, 1405 (C=N). 1601 (C=C). 1714 (CHO).	6.9-8.3 (m, 5H, aromatic). 10.8 (b, 2H, 2CHO). M <sup>+</sup> : 281
3a	691, 756 (monosubstituted phenyl). 1119 (C—O—C cyclic). 1363 (C—N). 1497, 1443 (C=N). 1600 (C=C). 1713 (CHO).	5.2 (b, 2H, 2 —CH=). 6.8-8.2 (m, 5H, aromatic). 9.5 (b, 2H, 2CHO).
4a	650, 691, 756 (monosubstituted phenyl). 1145 (C—O—C cyclic). 1362 (C—N). 1497, 1443 (C=N). 1598 (C=C). 1712 (CHO).	5.2 (b, 4H, 4 —CH=). 7-8.2 (m, 5H, aromatic). 10.5 (b, 2H, 2CHO).
5b	690, 755 (monosubstituted phenyl). 1116 (C—O—C cyclic). 1362 (C—N). 1495, 1445 (C=N). 1598 (C=C). 1714 (C=O).	1.1-2.4 (m, 6H, 2CH <sub>3</sub> of acetyl). 5.5 (b, 1H, 1 —CH=). 6.9-8.2 (m, 5H, aromatic). 9.5 (b, 1H, CHO).
6b	647, 690, 755 (monosubstituted phenyl). 1120, 1162 (C—O—C cyclic). 1312, 1363 (C—N). 1496, 1447(C=N). 1598 (C=C). 1715 (C=O).	0.8-2.4 (m, 6H, 2CH <sub>3</sub> of position 5). 3-4 (m, 6H, 2CH <sub>3</sub> of position 3). 7-8.2 (m, 5H, aromatic).
7	635, 692, 754 (monosubstituted phenyl). 1067 (C—O—C cyclic). 1365 (C—N). 1495, 1440 (C=N). 1597 (C=C). 1717 (C=O). 3424 (NH).	1.4-2.4 (m, 1H, NH of position 1 in hydantoin ring). 3-3.9 (m, 1H, NH of position 3 in hydantoin ring). 4.6-5.4 (m, 1H, —CH=). 6.9-8.2 (m, 5H, aromatic). 10.0 (s, 1H, CHO).
8	634, 722, 754 (monosubstituted phenyl). 1067, 1198 (C—O—C cyclic). 1494, 1434(C=N). 1600 (C=C). 1707, 1779 (C=O). 3404 (NH).	1.4-2.4 (m, 2H, 2NH of position 1 in hydantoin ring). 3-4.0 (m, 2H, 2NH of position 3 in hydantoin ring). 4.6-5.4 (m, 2H, 2 —CH=). 6.8-8.2 (m, 5H, aromatic).

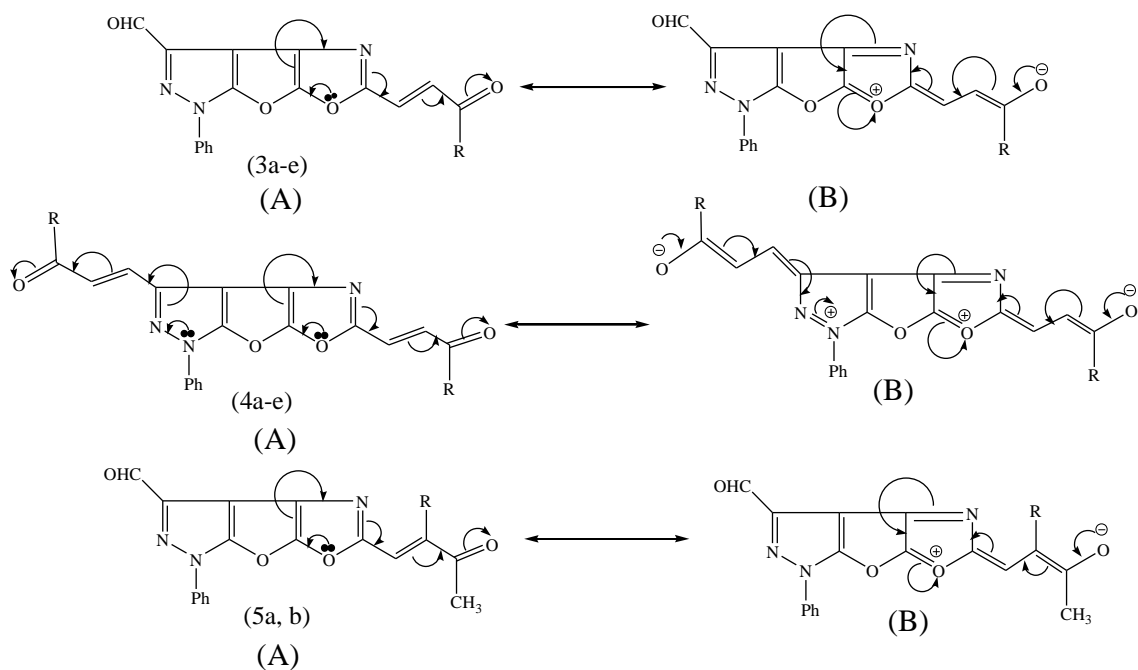


Scheme (1)

Synthesis Strategy of the prepared compounds (2), (3a-e), (4a-e), (5a, b), (6a, b), (7), and (8).

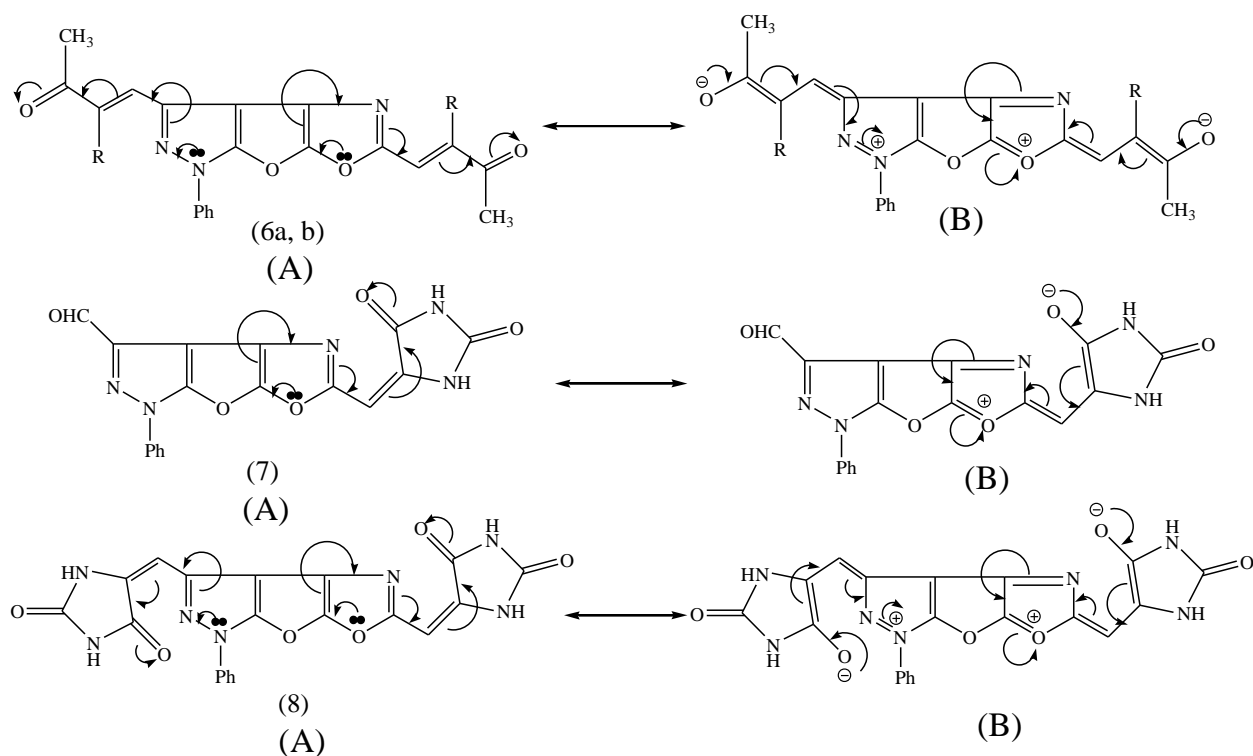
**Substituents in scheme (1):**

(3a-e), (4a-e): R = H (a), CH<sub>3</sub> (b), Ph (c), C<sub>6</sub>H<sub>4</sub>.p.OCH<sub>3</sub> (d), C<sub>6</sub>H<sub>4</sub>.p.NO<sub>2</sub> (e).  
 (5a, b), (6a, b): R = COOEt (a), COCH<sub>3</sub> (b)



Scheme (2)

Colour intensity and / or the electronic charge transfer pathways illustration of the synthesized acyclic merocyanine dyes (3a-e), (4a-e), (5a, b).



Scheme (2) continue

Colour intensity and / or the electronic charge transfer pathways illustration of the synthesized acyclic merocyanine dyes (6a, b) and cyclic merocyanine dyes (7), (8).